Dielectric Measurements on Thin Film (LiNbO3; SiPt)

Physics Advanced Labs by Professor António Onofre

Britta Dorn

Marco Brito

Rafael Cerqueira

Outline

- Introduction- Know how to produce and study thin films
- Mathematical details- What we need to know for dielectric data analysis
- Data analysis- Learn to fit in Origin in physical analysis context
- Discussion and conclusion

Introduction

Thin Films

- In the past, present and in future we have used and will use thin films in our daily life from low to high tech devices.
- What is a thin film? It is a set of atomic layers (in the order of nanometers) that are deposited on a substrate. Due to tensile or epitaxial strains we can change the different physical properties of the materials.
- The positive aspect of this is, we can have the following:
  - Small Size;
  - Economic value;
  - Functionality;

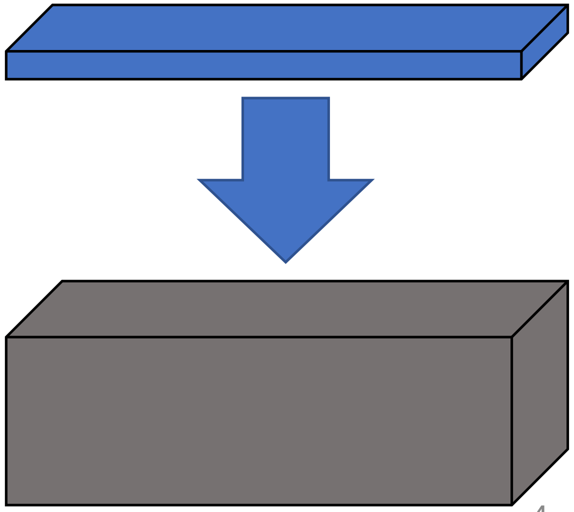

Utilities and applications

Solar cells;

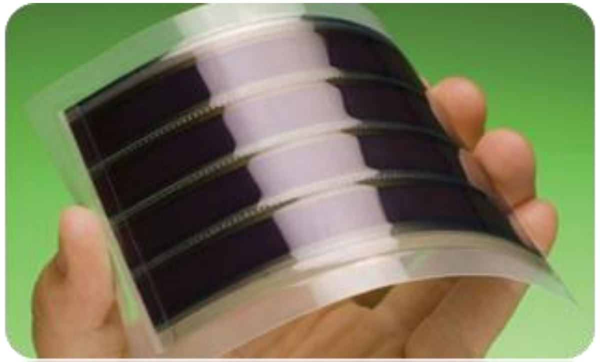

Glasses

Batteries

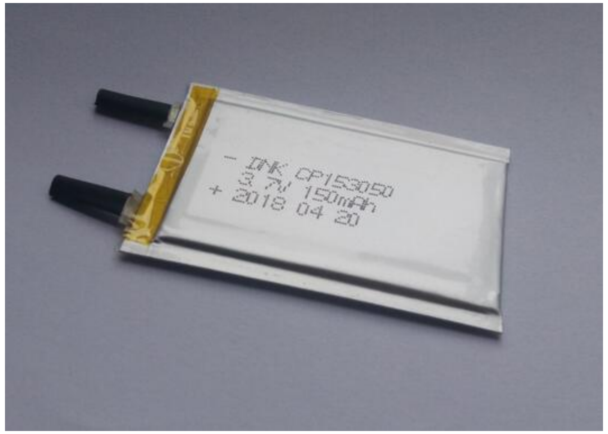

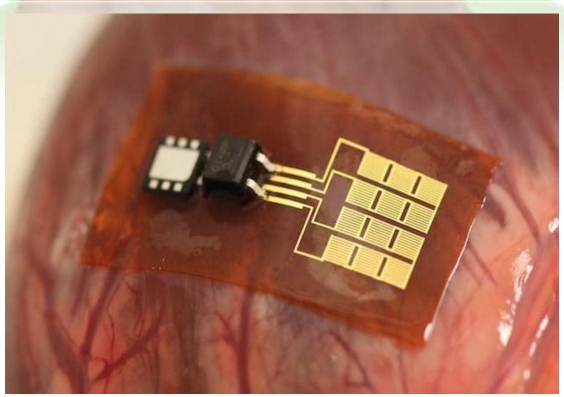

Medical Devices

Hard disk

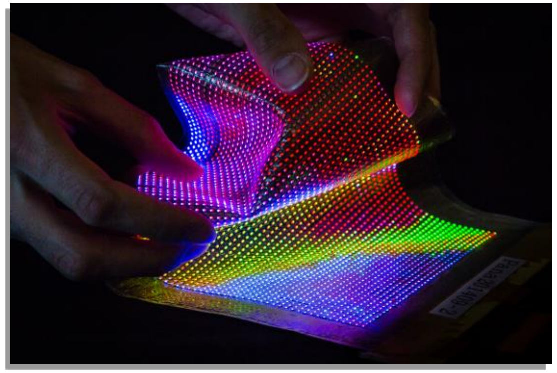

Screens

PLD- How to produce?

Experimental conditions:

-Deposition Temperature: 650°C

-O2 Pressure: 1mbar

-Deposition Time: 45 minutes

-Laser Energy: 350 mJ

-Laser Frequency: 6 Hz

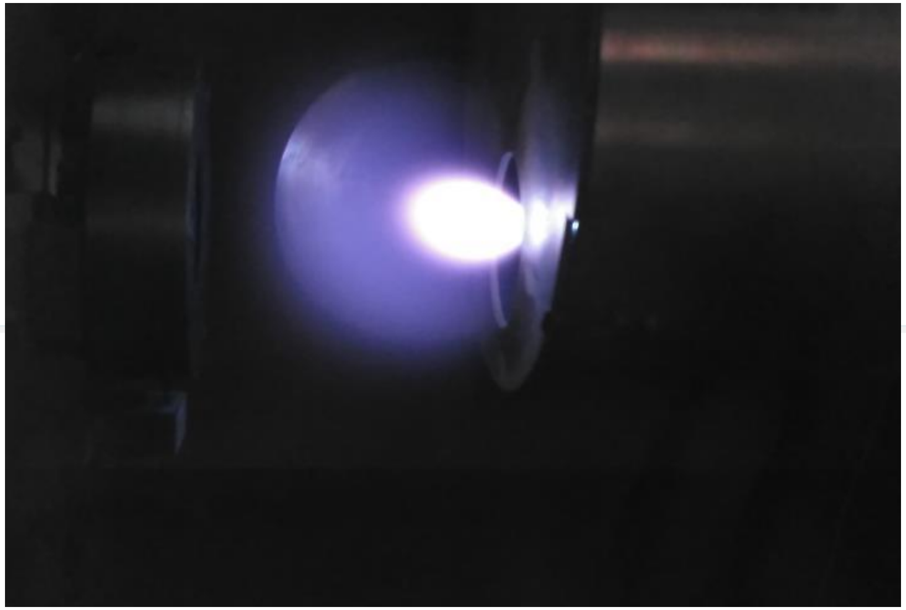

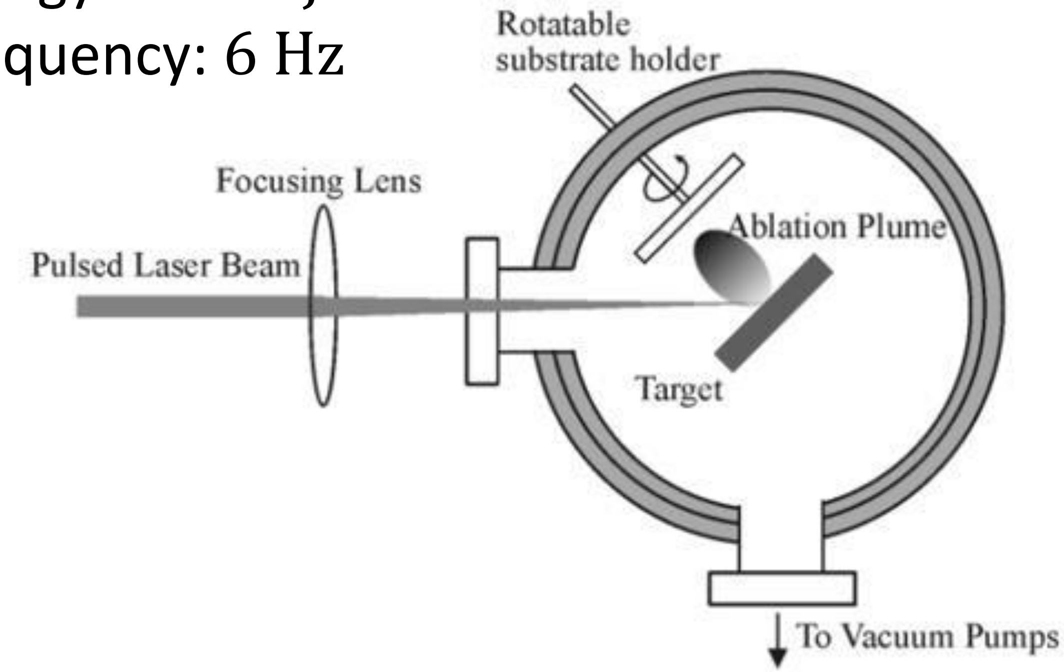

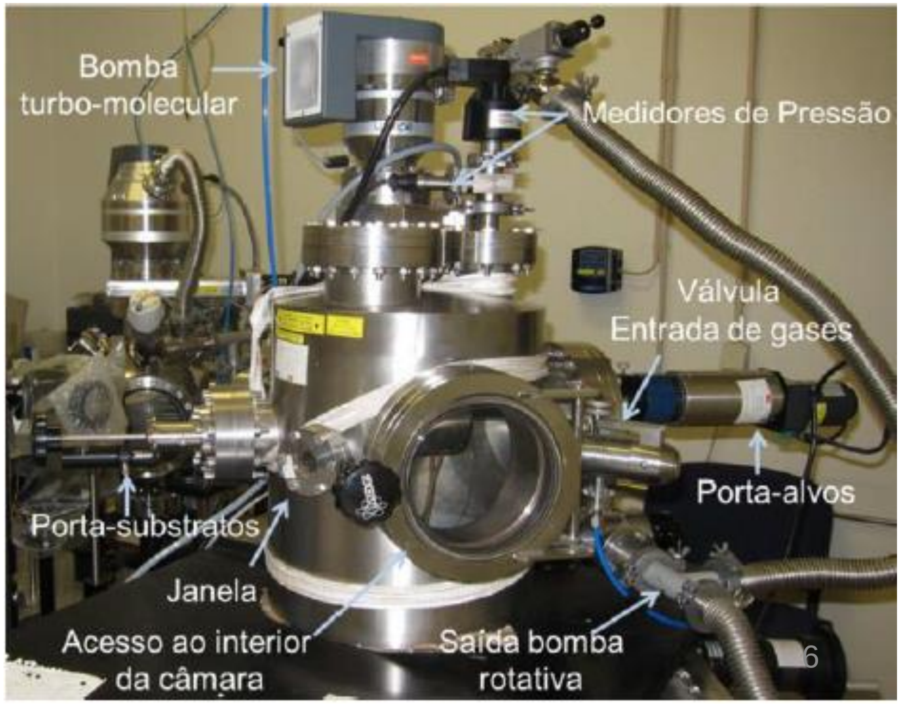

LiNbO3

- Professor Bernardo and his PhD students Bruna and João wanted to make thin films and study their physical properties.
- They chose $LiNbO_3$ as a film and PtSi(001) as substrate due to the wide range of physical properties exhibited by $LiNbO_3$.

LiNbO3 ID Card

- Physical properties: ferroelectric material, high piezoelectric, pyroelectric, electro-optical, birefringent, photorefractive and photoelastic properties.
- Structure: rhombohedral (R3c)
- Lattice parameters: $a = 5{,}1494$ Å and $c = 13{,}862$ Å
- Currie Temperature: $1{,}530\text{K}$
- Molar Mass: $147{,}846\ \text{g/mol}$
- Band Gap: 4eV

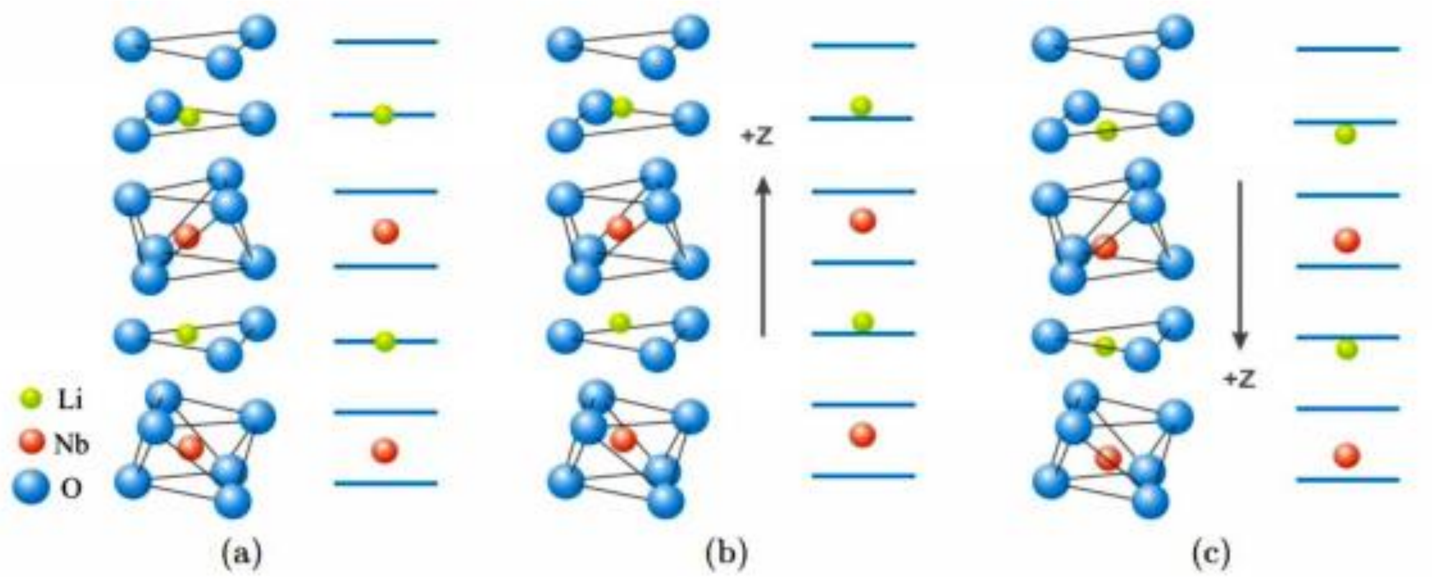

Figure 1: Atomic structure of LiNbO3 in (a) paraelectric phase and (b, c) ferroelectric phases[2].

LiNbO3- Utilities and applications

- Piezoeletric Devices

Waveguides

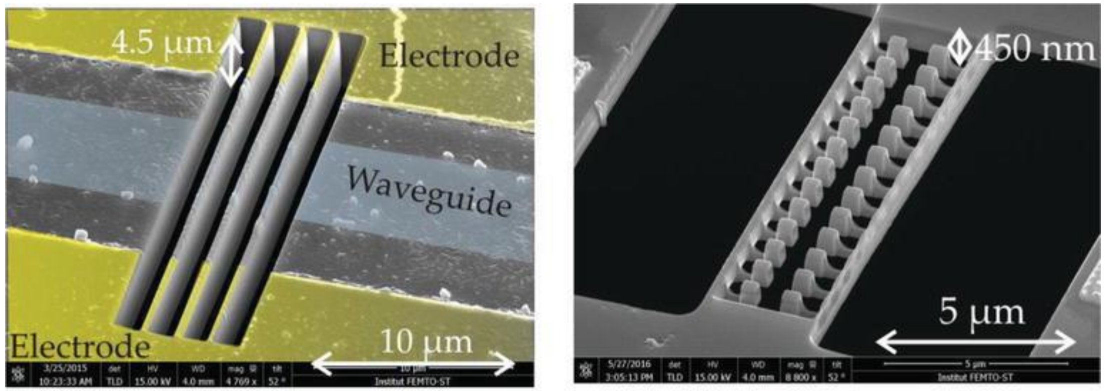

(a) (b)

Optical Modulators

Ferroelectric Effect

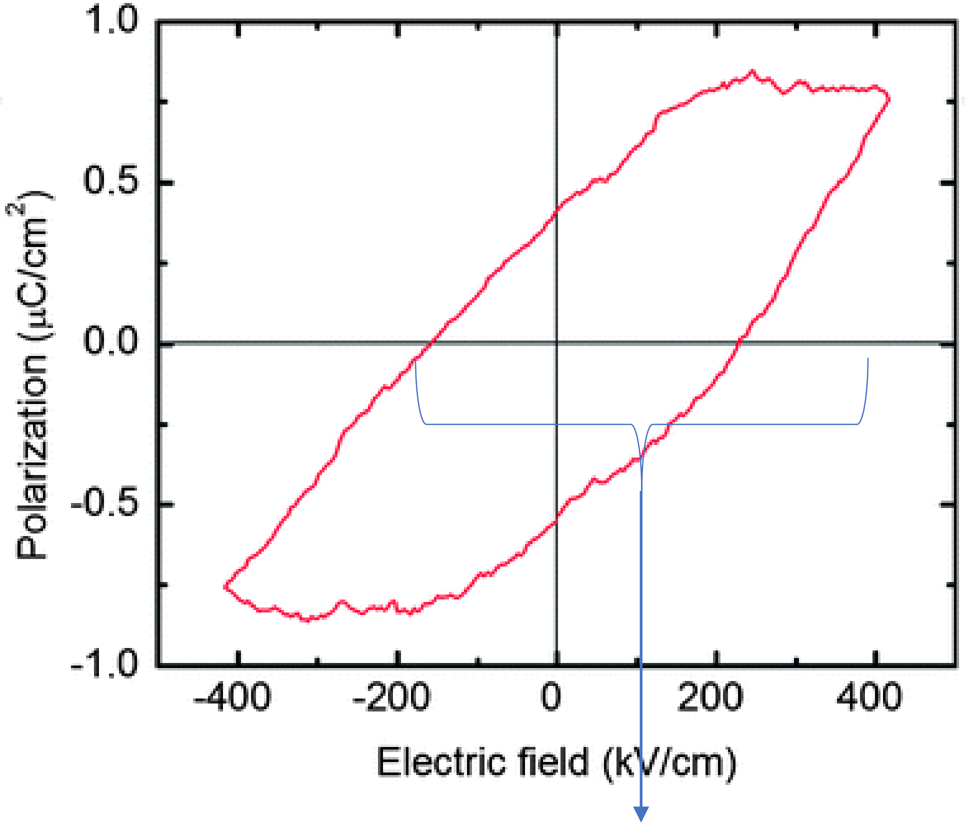

Relaxion Time

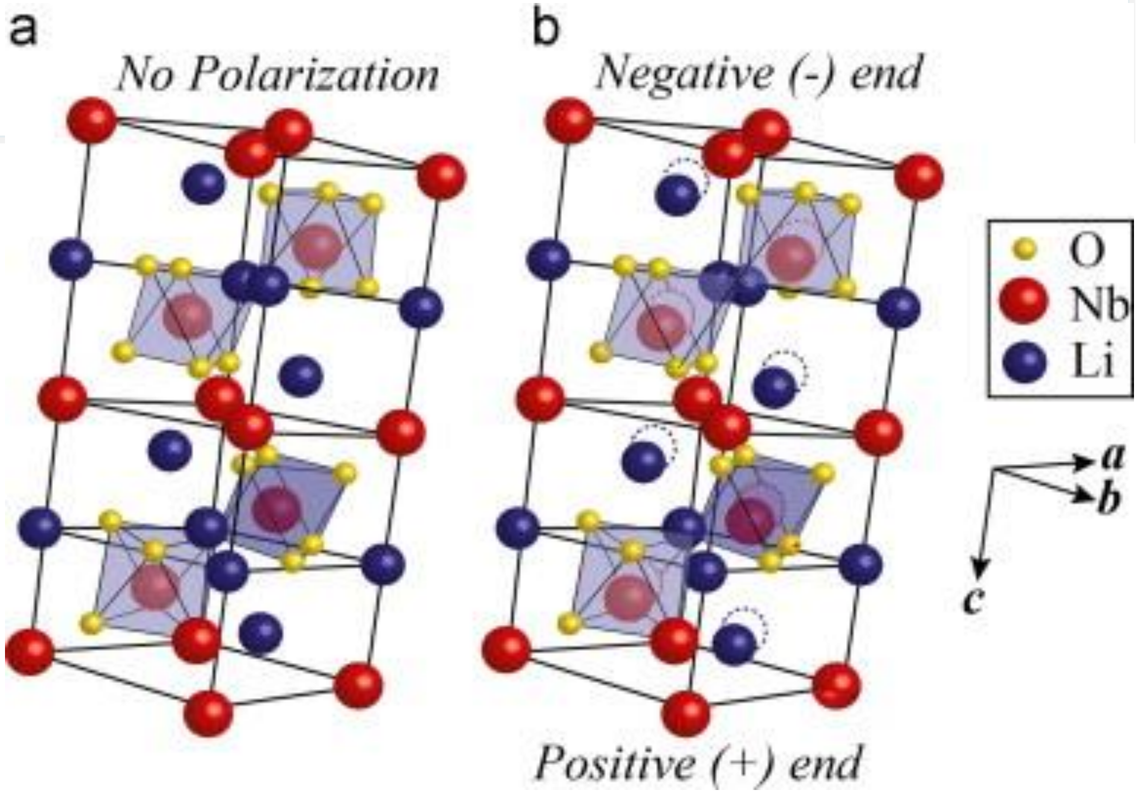

How to measure dielectric data?

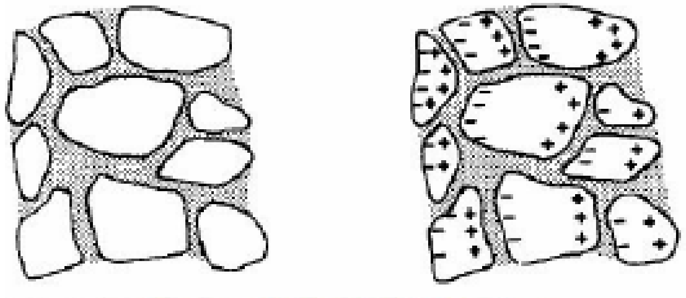

Various polarization processes.

- To know better the electric properties we need to measure the dielectric data with an impedance analyser.

Impedance analyzer:
- Waine Kerr 6440 A;
- frequency range:10Hz - 3MHz;

Temperature controller and furnace:
- Polymer Labs PL706 PID;
- temperatures of $15 - 200°C$ ($50°C$ in our case);
- 2ºC/min temperature measurement;

Software:
- Labview;

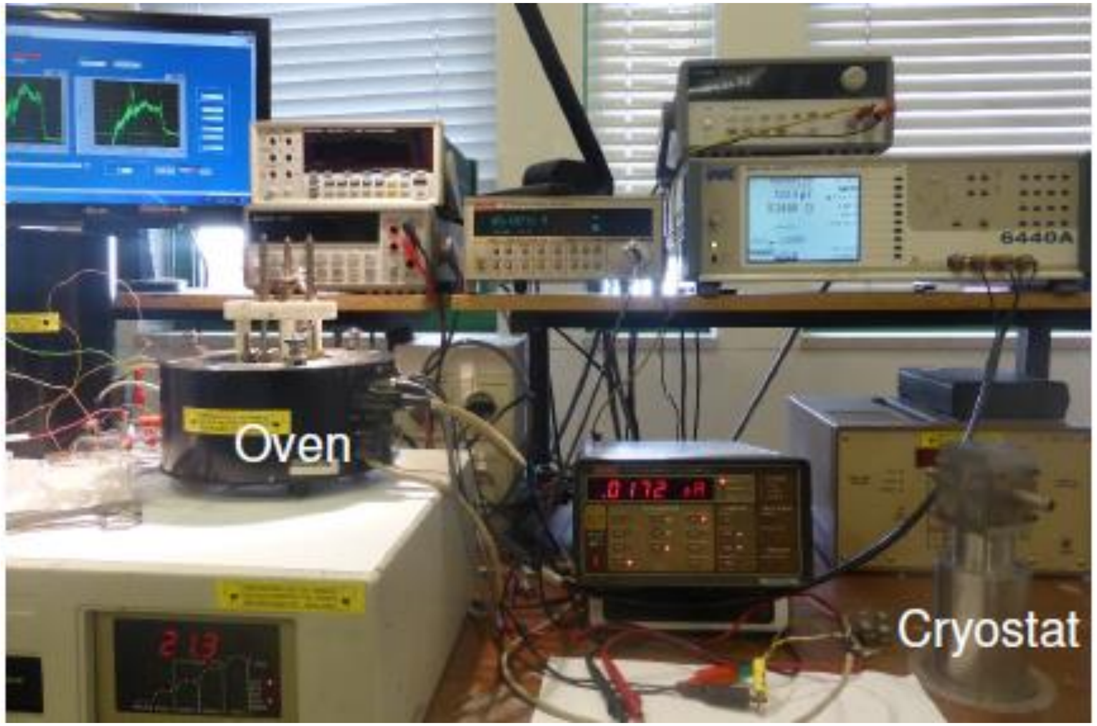

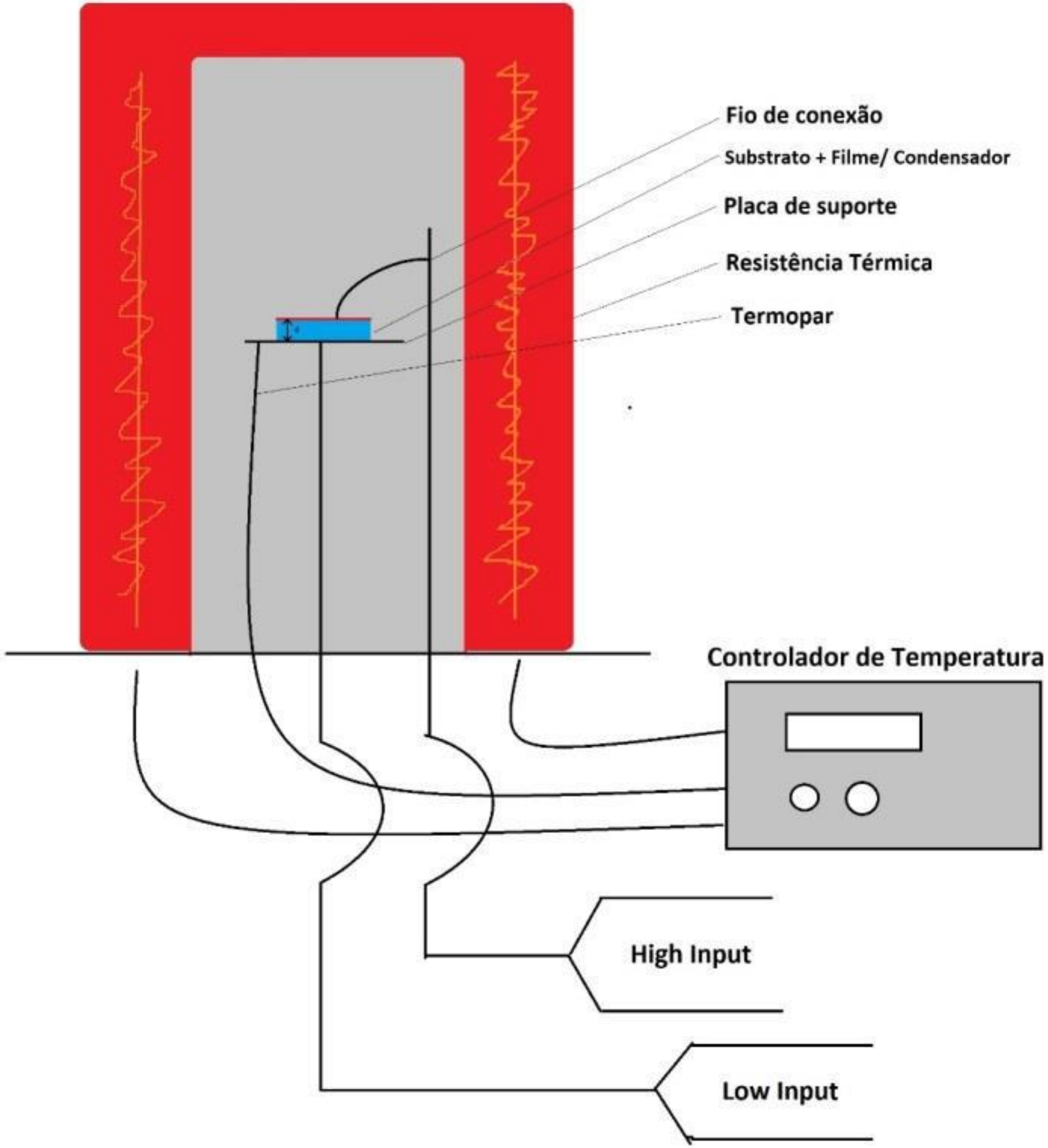
Fio de conexão
Substrato + Filme/ Condensador
Placa de suporte
Resistência Térmica
Termopar
Controlador de Temperatura
High Input
Low Input

Mathematical details

Dielectric function

- The susceptibility of a material is a measure of the electrical polarizability of the said material. For example in linear dielectrics, the polarization is given by: $\mathbf{P} = \epsilon_0 \chi \mathbf{E}$,
- The electric displacement field which describes the field produced by free charges is given by: $\mathbf{D} = \epsilon_0 \mathbf{E} + \mathbf{P} = \epsilon_0 (\mathbf{E} + \chi \mathbf{E}) = \epsilon_0 (1 + \chi) \mathbf{E}.$
- The permittivity of a material is then: $\epsilon = \epsilon_0 (1 + \chi) .$
- The dielectric function is defined as $\epsilon_r = \frac{\epsilon}{\epsilon_0}.$

Dielectric function

- For example in the vacuum the dielectric function is $\epsilon_r = \frac{\epsilon}{\epsilon_0} = \frac{\epsilon_0}{\epsilon_0} = 1$ while for other materials is >1.
- For nonlinear materials and anisotropic materials the dielectric function might be a highly nonlinear equation and dependent on the frequency of the electric field and might not be a scalar but a tensor.
- There are several models for the dielectric functions of a material.

Havriliak-Negami model

- In this model the dielectric function is given by $\epsilon(\omega) = \epsilon_\infty + \frac{\Delta\epsilon}{(1 + (\mathrm{i}\omega\tau_{HN})^\alpha)^\beta}$
- It can be divided in its real and imaginary parts given by

$$\Re(\epsilon) = \epsilon' = \Delta\epsilon r(\omega)\cos\left[\gamma\psi(\omega)\right] + \epsilon_\infty;\ \Im(\epsilon) = \epsilon'' = \Delta\epsilon r(\omega)\sin\left[\gamma\psi(\omega)\right]$$

where

$$r(\omega) = \left[1 + 2\left(\omega\tau_{HN}\right)^\beta \cos\left(\frac{\beta\pi}{2}\right) + \left(\omega\tau_{HN}\right)^{2\beta}\right]^{-\gamma/2}$$

$$\psi(\omega) = \arctan\left[\frac{\sin\left(\beta\pi/2\right)}{\left(\omega\tau_{HN}\right)^{-\beta} + \cos\left(\beta\pi/2\right)}\right]$$

Havriliak-Negami model

- Moreover it is known that the dielectric function is dependent of some experimental parameters

$$\epsilon' = \frac{C \cdot d}{A}$$

$$\epsilon'' = \epsilon' \tan \delta$$

- The model can also be modified by two extra terms to correct the behavior of the function at low frequencies.
- For the real part we have the Maxwell-Wagner term $\frac{\mathcal{O}}{\omega^n}$ and for the imaginary part we have a term depending on the conductivity $\frac{\sigma}{\epsilon_0 \omega^n}$

Area measurement

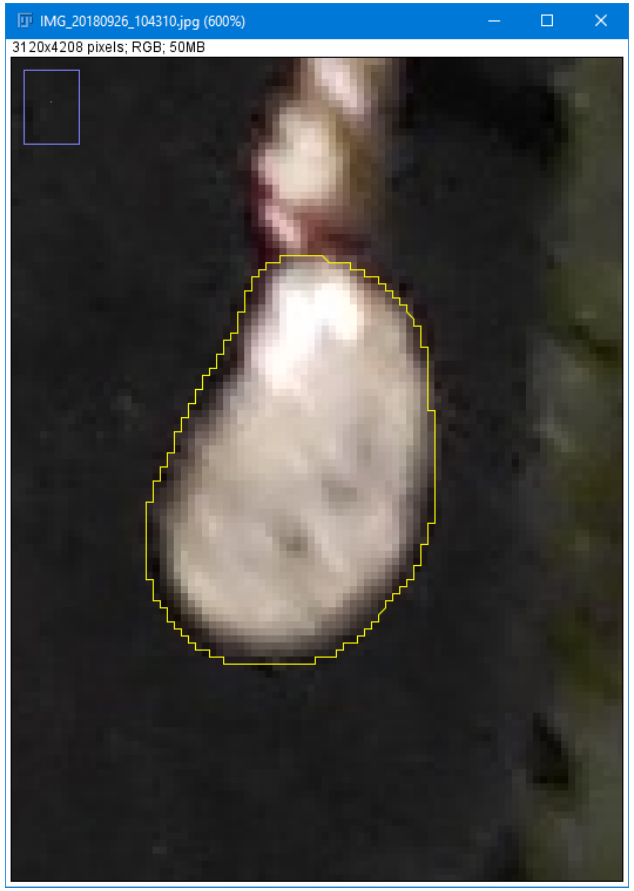

- Measurement of the area was done using the program “Image J“
- Using ruler for estimating length scale
- Final area is the average of 5 measurements
- $\bar{A} = 1{,}569 \times 10^{-6} \pm 3{,}69 \times 10^{-8}$
- About 2,4% uncertainty.

Uncertainties

$$\Delta C = 0.01C$$
$$\Delta \tan\delta = 0.01 \tan\delta$$
$$\Delta A = \text{standard deviation of five mesurements}$$

As for the uncertainties in the dielectric function values they are calculated using the standard error propagation formula for a standard function *f*:

$$\Delta f = \sqrt{\left(\frac{\partial f}{\partial x_1}\Delta x_1\right)^2 + \left(\frac{\partial f}{\partial x_2}\Delta x_2\right)^2 + \cdots}$$

Data Treatment and analysis

Fitting

- Our objective is to fit the experimental values of the dielectric function to the Havriliak-Negami model and if necessary, add extra corrective terms.

Fits without uncertainties

Imaginary and real part individual fit

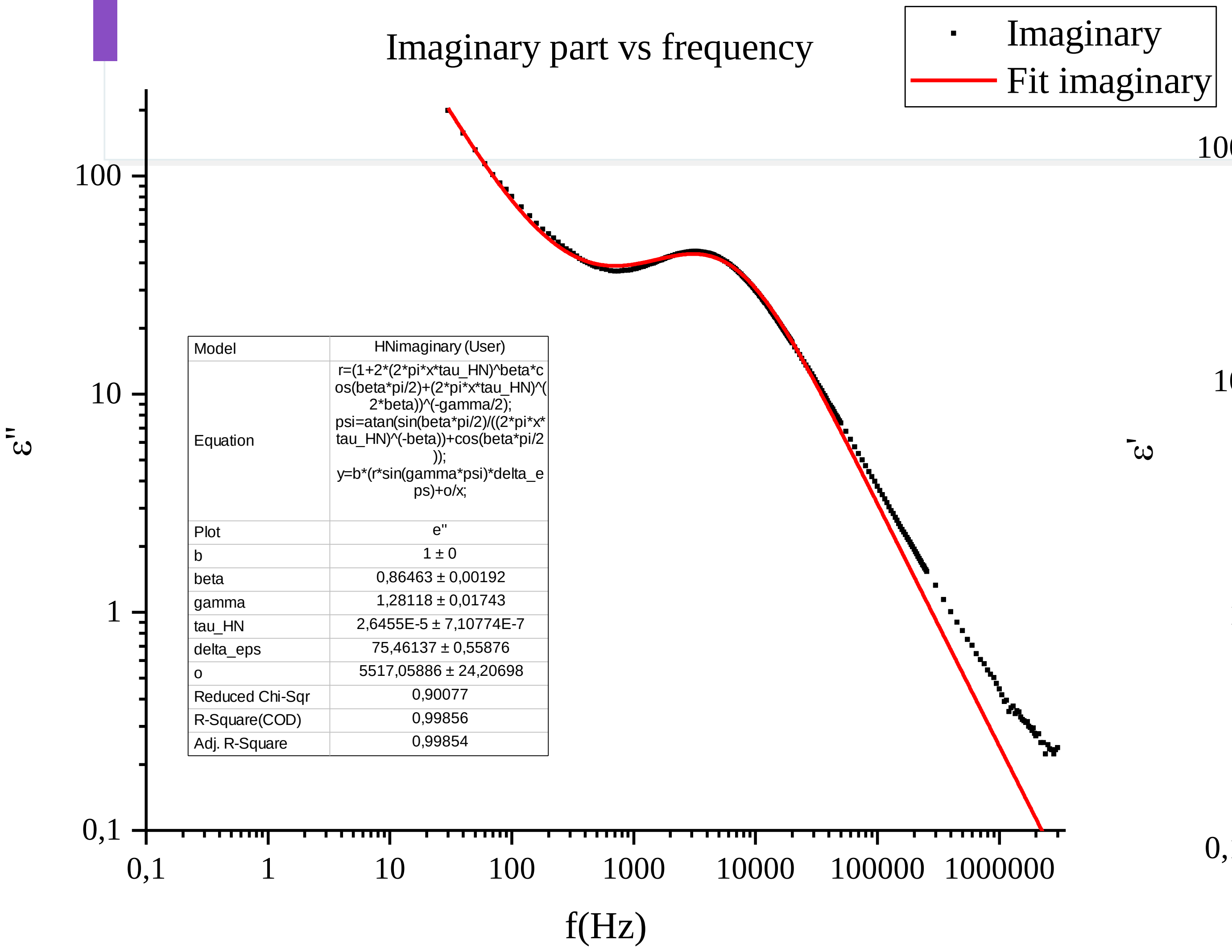

Model	HNimaginary (User)
Equation	r=(1+2*(2*pi*x*tau_HN)^beta*cos(beta*pi/2)+(2*pi*x*tau_HN)^(2*beta))^(-gamma/2); psi=atan(sin(beta*pi/2)/((2*pi*x*tau_HN)^(-beta))+cos(beta*pi/2)); y=b*(r*sin(gamma*psi)*delta_eps)+o/x;
Plot	e''
b	1 ± 0
beta	0,86463 ± 0,00192
gamma	1,28118 ± 0,01743
tau_HN	2,6455E-5 ± 7,10774E-7
delta_eps	75,46137 ± 0,55876
o	5517,05886 ± 24,20698
Reduced Chi-Sqr	0,90077
R-Square(COD)	0,99856
Adj. R-Square	0,99854

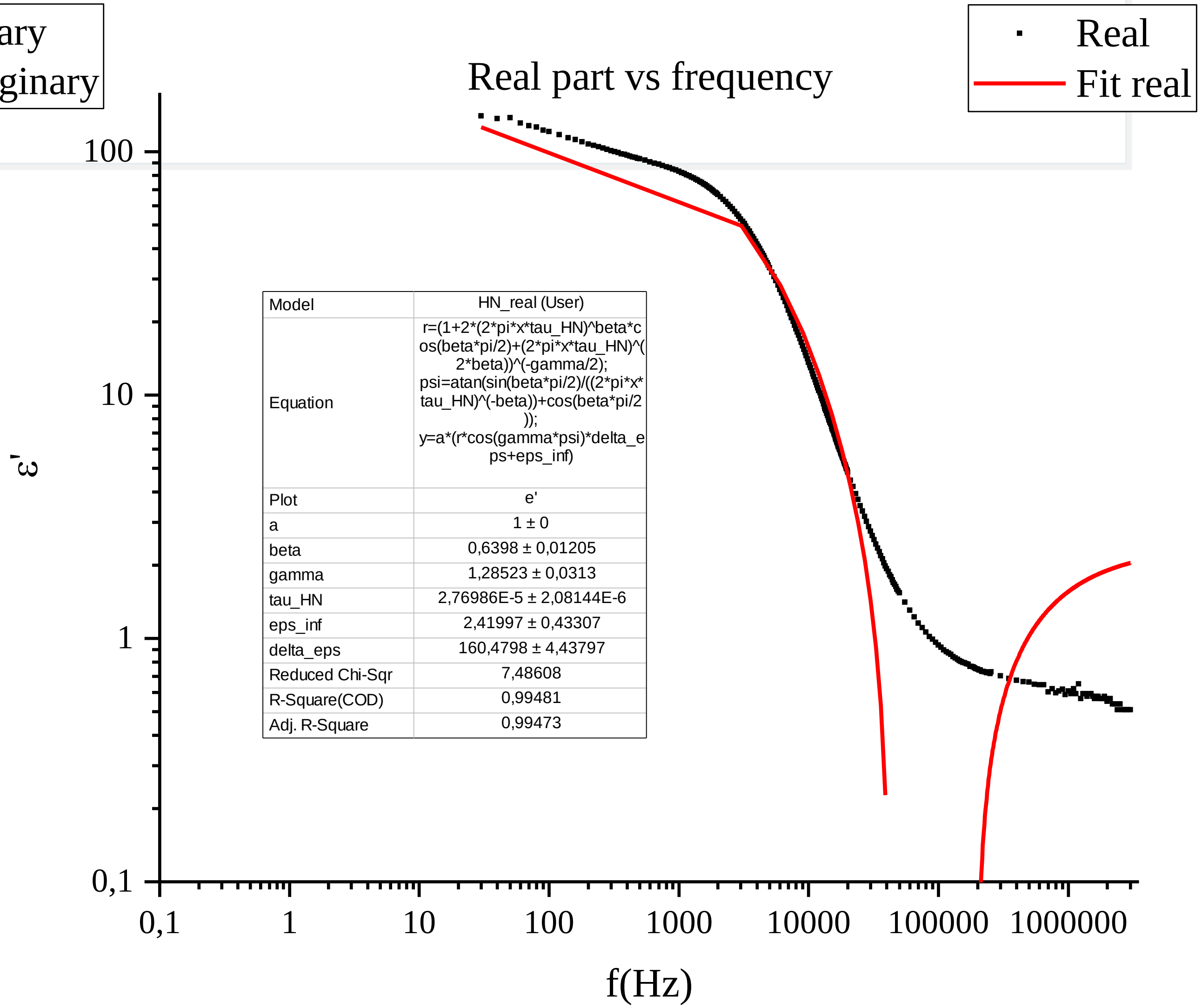

Model	HN_real (User)
Equation	r=(1+2*(2*pi*x*tau_HN)^beta*cos(beta*pi/2)+(2*pi*x*tau_HN)^(2*beta))^(-gamma/2); psi=atan(sin(beta*pi/2)/((2*pi*x*tau_HN)^(-beta))+cos(beta*pi/2)); y=a*(r*cos(gamma*psi)*delta_eps+eps_inf)
Plot	e'
a	1 ± 0
beta	0,6398 ± 0,01205
gamma	1,28523 ± 0,0313
tau_HN	2,76986E-5 ± 2,08144E-6
eps_inf	2,41997 ± 0,43307
delta_eps	160,4798 ± 4,43797
Reduced Chi-Sqr	7,48608
R-Square(COD)	0,99481
Adj. R-Square	0,99473

Global fit – No corrections

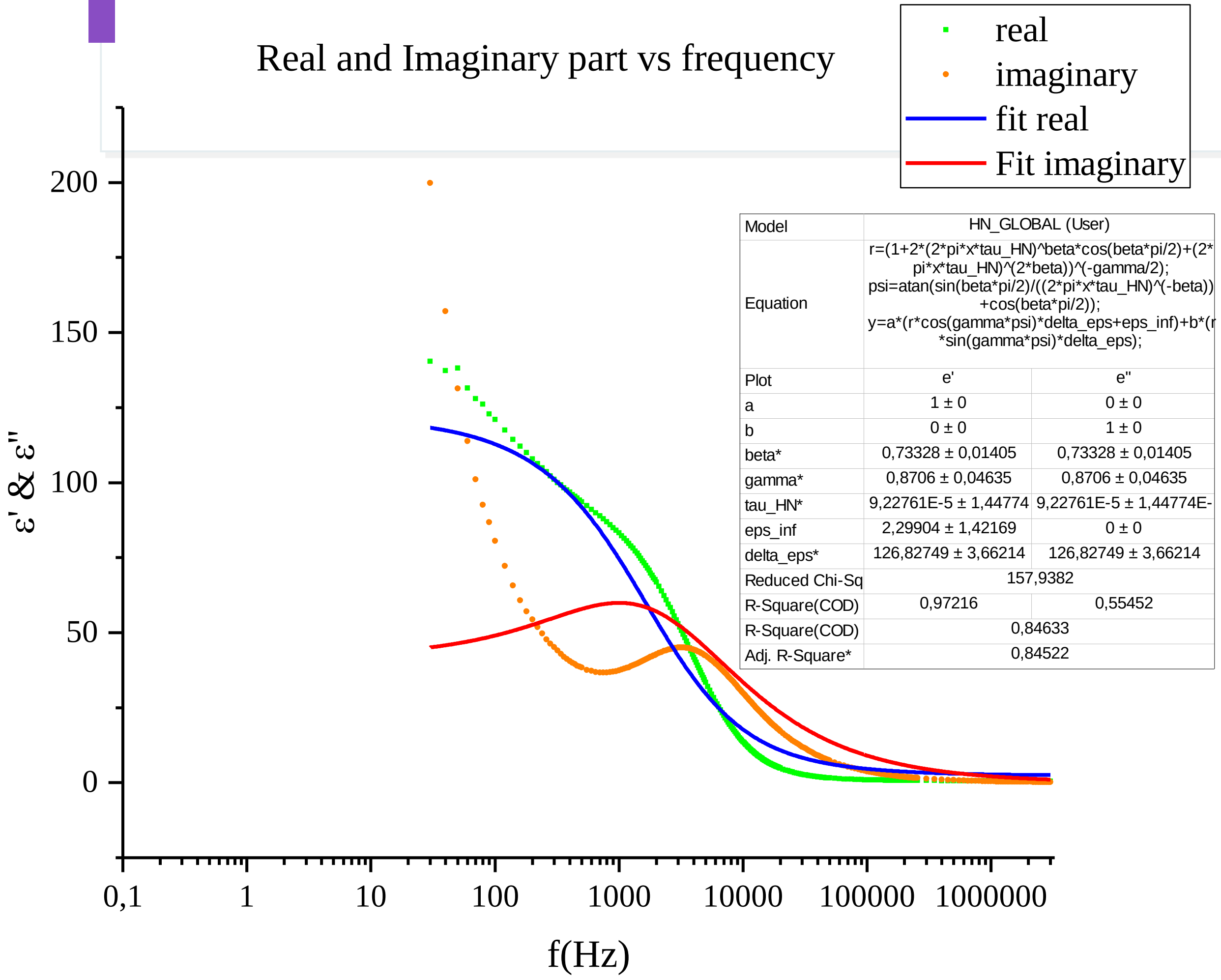

Model	HN_GLOBAL (User)	
Equation	r=(1+2*(2*pi*x*tau_HN)^beta*cos(beta*pi/2)+(2*pi*x*tau_HN)^(2*beta))^(-gamma/2); psi=atan(sin(beta*pi/2)/((2*pi*x*tau_HN)^(-beta))+cos(beta*pi/2)); y=a*(r*cos(gamma*psi)*delta_eps+eps_inf)+b*(r*sin(gamma*psi)*delta_eps);	
Plot	e'	e''
a	1 ± 0	0 ± 0
b	0 ± 0	1 ± 0
beta*	0,73328 ± 0,01405	0,73328 ± 0,01405
gamma*	0,8706 ± 0,04635	0,8706 ± 0,04635
tau_HN*	9,22761E-5 ± 1,44774	9,22761E-5 ± 1,44774E-
eps_inf	2,29904 ± 1,42169	0 ± 0
delta_eps*	126,82749 ± 3,66214	126,82749 ± 3,66214
Reduced Chi-Sq	157,9382	
R-Square(COD)	0,97216	0,55452
R-Square(COD)	0,84633	
Adj. R-Square*	0,84522	

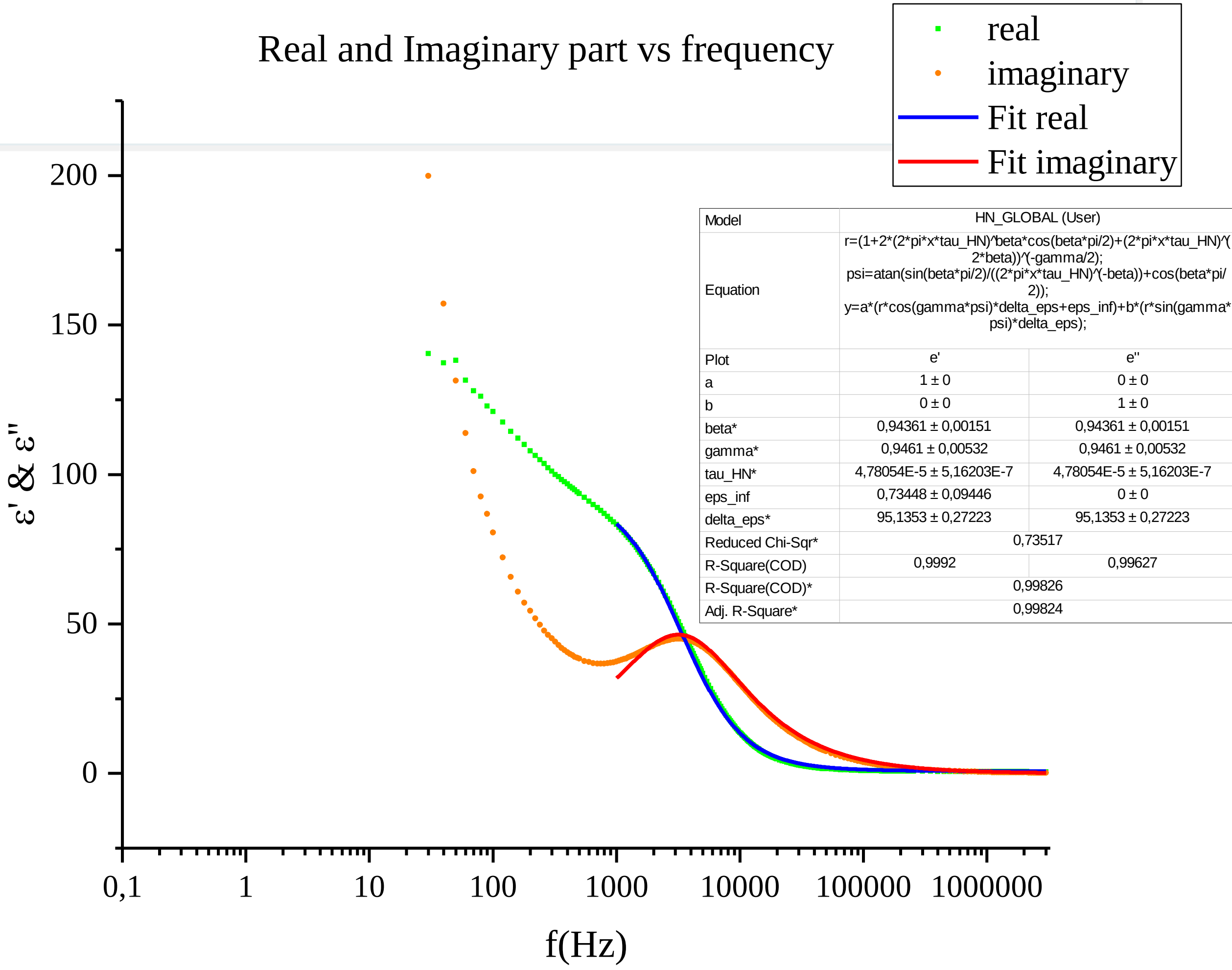

Model	HN_GLOBAL (User)	
Equation	r=(1+2*(2*pi*x*tau_HN)^beta*cos(beta*pi/2)+(2*pi*x*tau_HN)^(2*beta))^(-gamma/2); psi=atan(sin(beta*pi/2)/((2*pi*x*tau_HN)^(-beta))+cos(beta*pi/2)); y=a*(r*cos(gamma*psi)*delta_eps+eps_inf)+b*(r*sin(gamma*psi)*delta_eps);	
Plot	e'	e''
a	1 ± 0	0 ± 0
b	0 ± 0	1 ± 0
beta*	0,94361 ± 0,00151	0,94361 ± 0,00151
gamma*	0,9461 ± 0,00532	0,9461 ± 0,00532
tau_HN*	4,78054E-5 ± 5,16203E-7	4,78054E-5 ± 5,16203E-7
eps_inf	0,73448 ± 0,09446	0 ± 0
delta_eps*	95,1353 ± 0,27223	95,1353 ± 0,27223
Reduced Chi-Sqr*	0,73517	
R-Square(COD)	0,9992	0,99627
R-Square(COD)*	0,99826	
Adj. R-Square*	0,99824	

Global fits with real and imaginary corrections

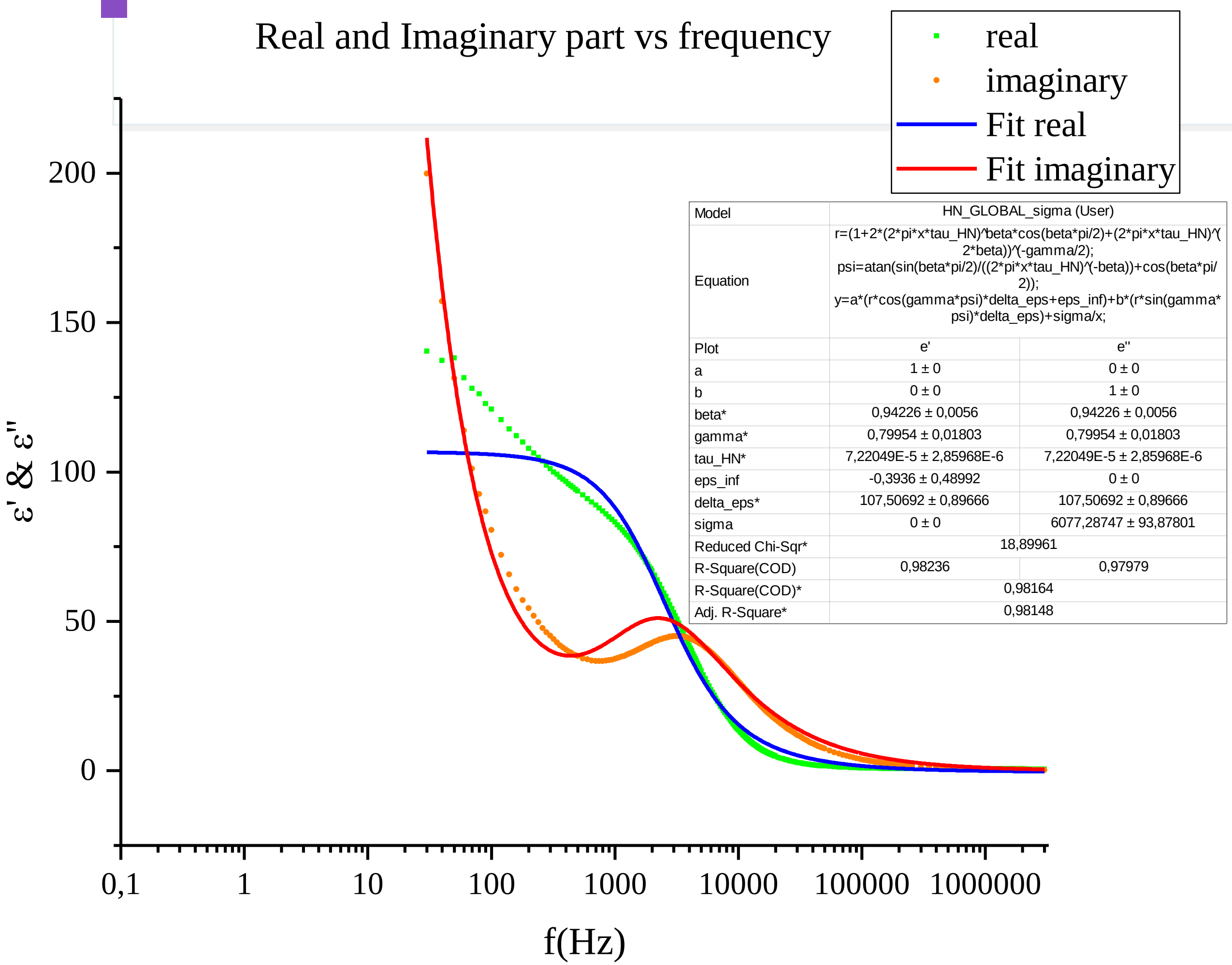

Model	HN_GLOBAL_sigma (User)	
Equation	r=(1+2*(2*pi*x*tau_HN)^beta*cos(beta*pi/2)+(2*pi*x*tau_HN)^(2*beta))^(-gamma/2); psi=atan(sin(beta*pi/2)/((2*pi*x*tau_HN)^(-beta))+cos(beta*pi/2)); y=a*(r*cos(gamma*psi)*delta_eps+eps_inf)+b*(r*sin(gamma*psi)*delta_eps)+sigma/x;	
Plot	e'	e''
a	1 ± 0	0 ± 0
b	0 ± 0	1 ± 0
beta*	0,94226 ± 0,0056	0,94226 ± 0,0056
gamma*	0,79954 ± 0,01803	0,79954 ± 0,01803
tau_HN*	7,22049E-5 ± 2,85968E-6	7,22049E-5 ± 2,85968E-6
eps_inf	-0,3936 ± 0,48992	0 ± 0
delta_eps*	107,50692 ± 0,89666	107,50692 ± 0,89666
sigma	0 ± 0	6077,28747 ± 93,87801
Reduced Chi-Sqr*	18,89961	
R-Square(COD)	0,98236	0,97979
R-Square(COD)*	0,98164	
Adj. R-Square*	0,98148	

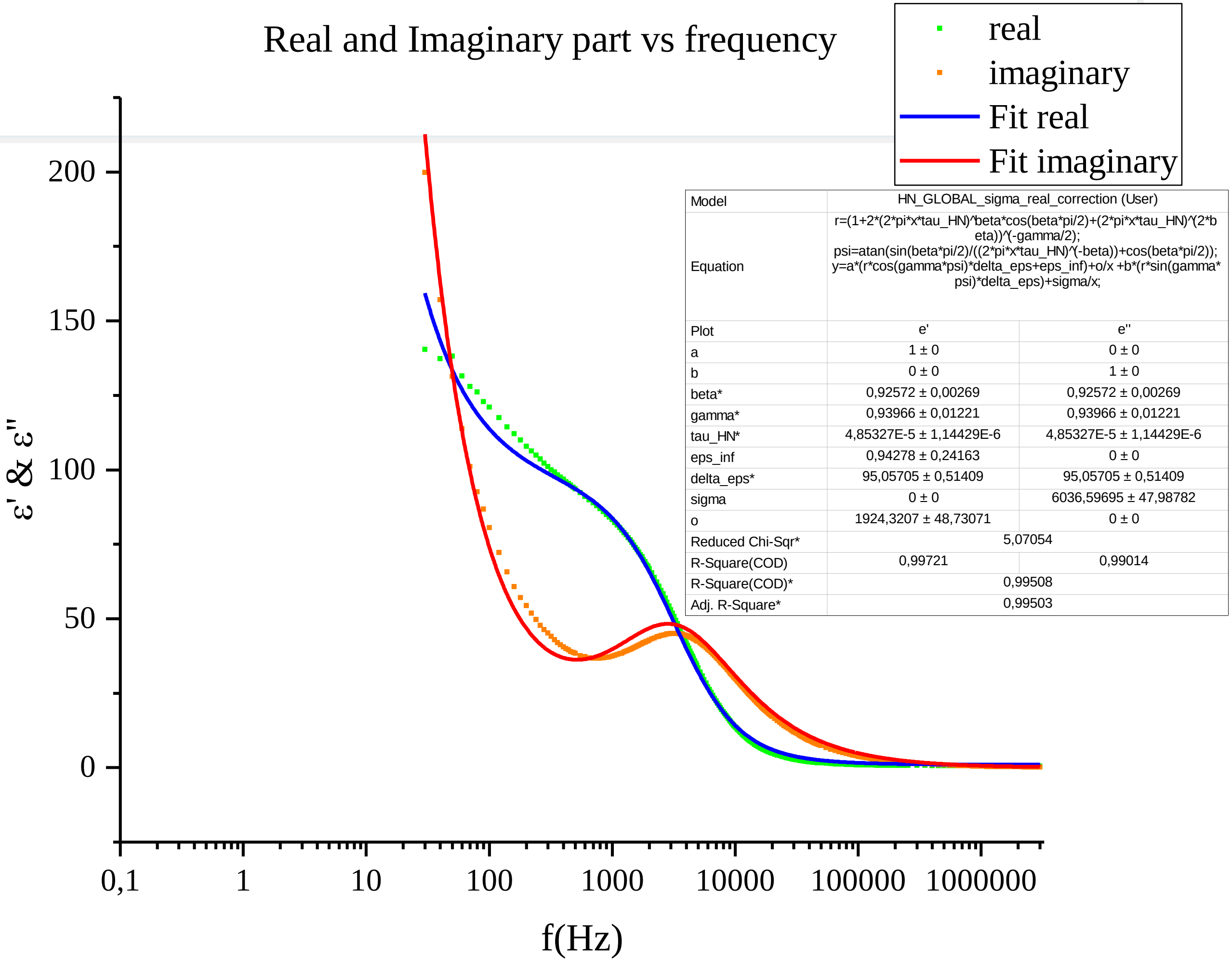

Model	HN_GLOBAL_sigma_real_correction (User)	
Equation	r=(1+2*(2*pi*x*tau_HN)^beta*cos(beta*pi/2)+(2*pi*x*tau_HN)^(2*beta))^(-gamma/2); psi=atan(sin(beta*pi/2)/((2*pi*x*tau_HN)^(-beta))+cos(beta*pi/2)); y=a*(r*cos(gamma*psi)*delta_eps+eps_inf)+o/x +b*(r*sin(gamma*psi)*delta_eps)+sigma/x;	
Plot	e'	e''
a	1 ± 0	0 ± 0
b	0 ± 0	1 ± 0
beta*	0,92572 ± 0,00269	0,92572 ± 0,00269
gamma*	0,93966 ± 0,01221	0,93966 ± 0,01221
tau_HN*	4,85327E-5 ± 1,14429E-6	4,85327E-5 ± 1,14429E-6
eps_inf	0,94278 ± 0,24163	0 ± 0
delta_eps*	95,05705 ± 0,51409	95,05705 ± 0,51409
sigma	0 ± 0	6036,59695 ± 47,98782
o	1924,3207 ± 48,73071	0 ± 0
Reduced Chi-Sqr*	5,07054	
R-Square(COD)	0,99721	0,99014
R-Square(COD)*	0,99508	
Adj. R-Square*	0,99503	

Global fit with corrections with exponents

Real and imaginary part vs frequency

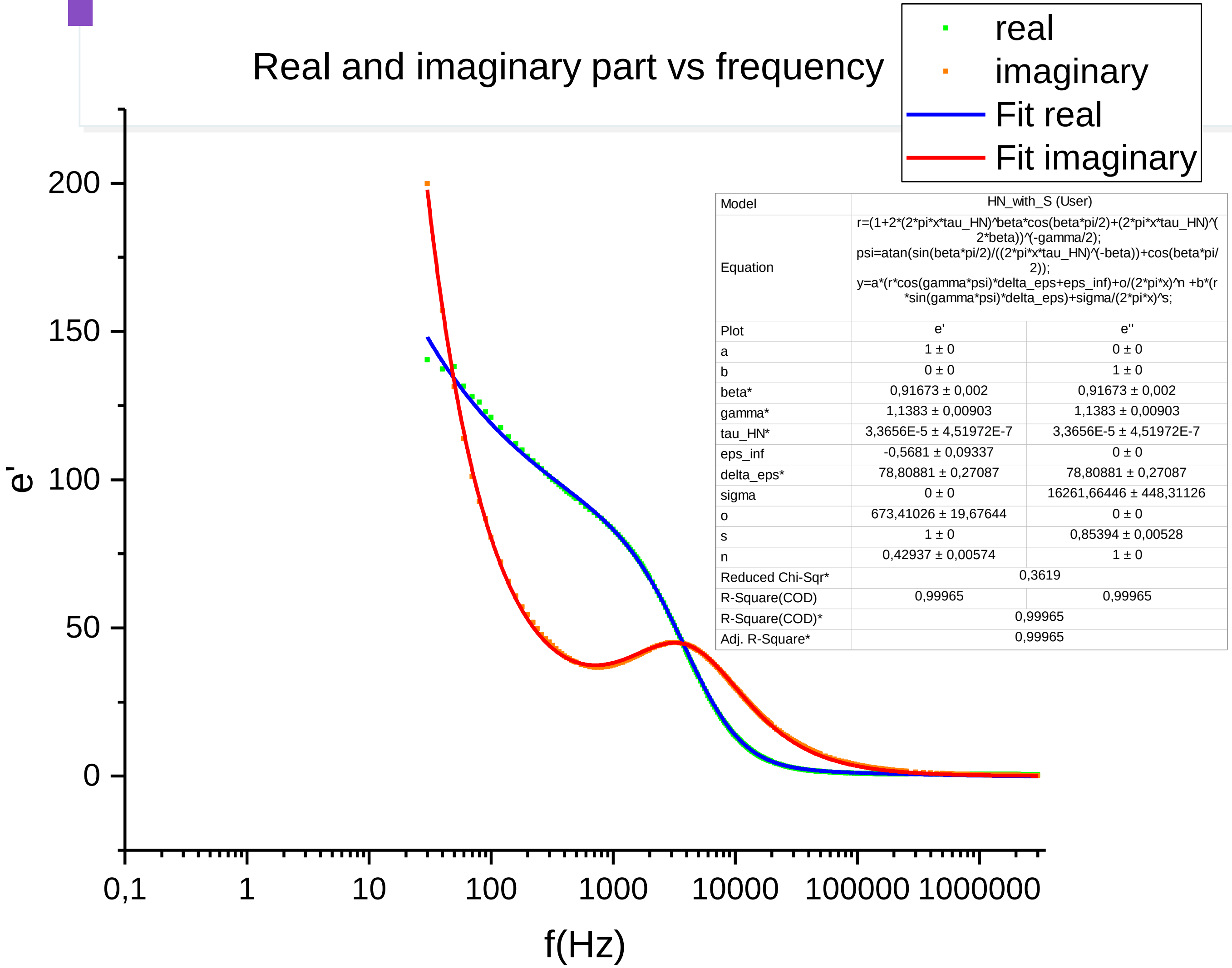

Model	HN_with_S (User)	

Equation	r=(1+2*(2*pi*x*tau_HN)^beta*cos(beta*pi/2)+(2*pi*x*tau_HN)^(2*beta))^(-gamma/2);
	psi=atan(sin(beta*pi/2)/((2*pi*x*tau_HN)^(-beta))+cos(beta*pi/2));
	y=a*(r*cos(gamma*psi)*delta_eps+eps_inf)+o/(2*pi*x)^n +b*(r*sin(gamma*psi)*delta_eps)+sigma/(2*pi*x)^s;	

Plot	e'	e''
a	1 ± 0	0 ± 0
b	0 ± 0	1 ± 0
beta*	0,91673 ± 0,002	0,91673 ± 0,002
gamma*	1,1383 ± 0,00903	1,1383 ± 0,00903
tau_HN*	3,3656E-5 ± 4,51972E-7	3,3656E-5 ± 4,51972E-7
eps_inf	-0,5681 ± 0,09337	0 ± 0
delta_eps*	78,80881 ± 0,27087	78,80881 ± 0,27087
sigma	0 ± 0	16261,66446 ± 448,31126
o	673,41026 ± 19,67644	0 ± 0
s	1 ± 0	0,85394 ± 0,00528
n	0,42937 ± 0,00574	1 ± 0
Reduced Chi-Sqr*	0,3619	
R-Square(COD)	0,99965	0,99965
R-Square(COD)*	0,99965	
Adj. R-Square*	0,99965	

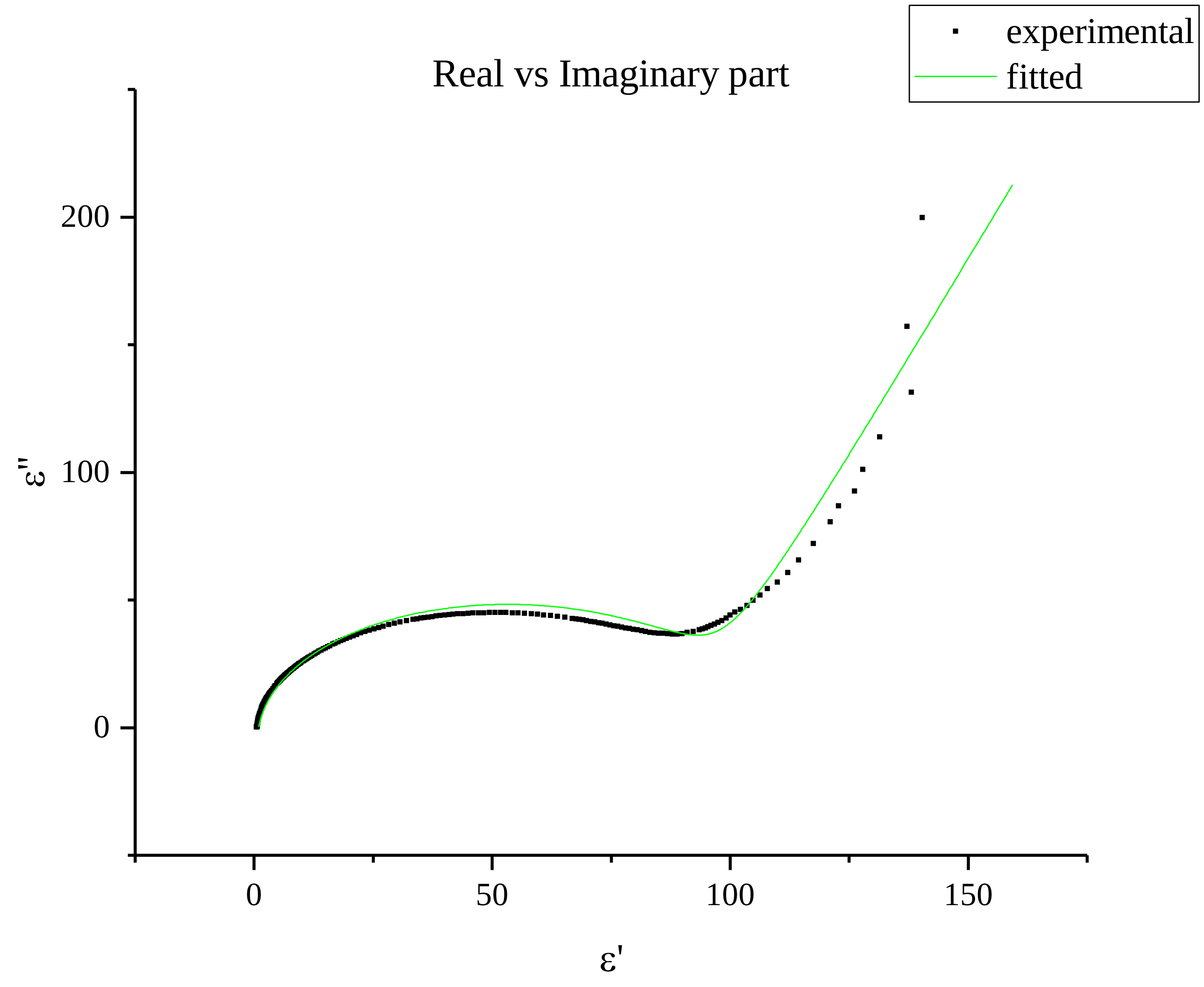

Real vs Imaginary part
experimental
fitted
ε''
200
100
0
0
50
100
150
ε'

Fits with uncertainties

Imaginary and real part individual fit

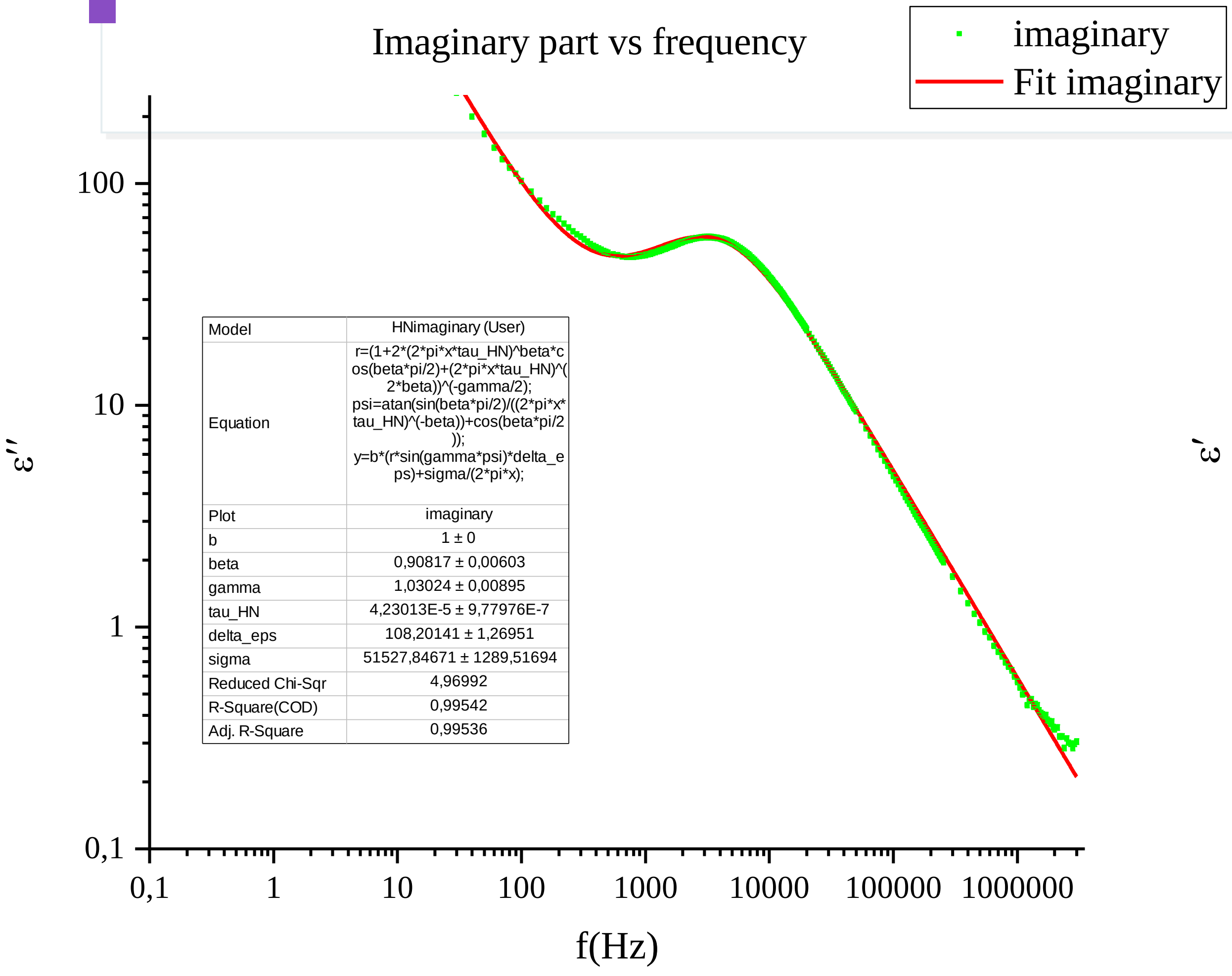

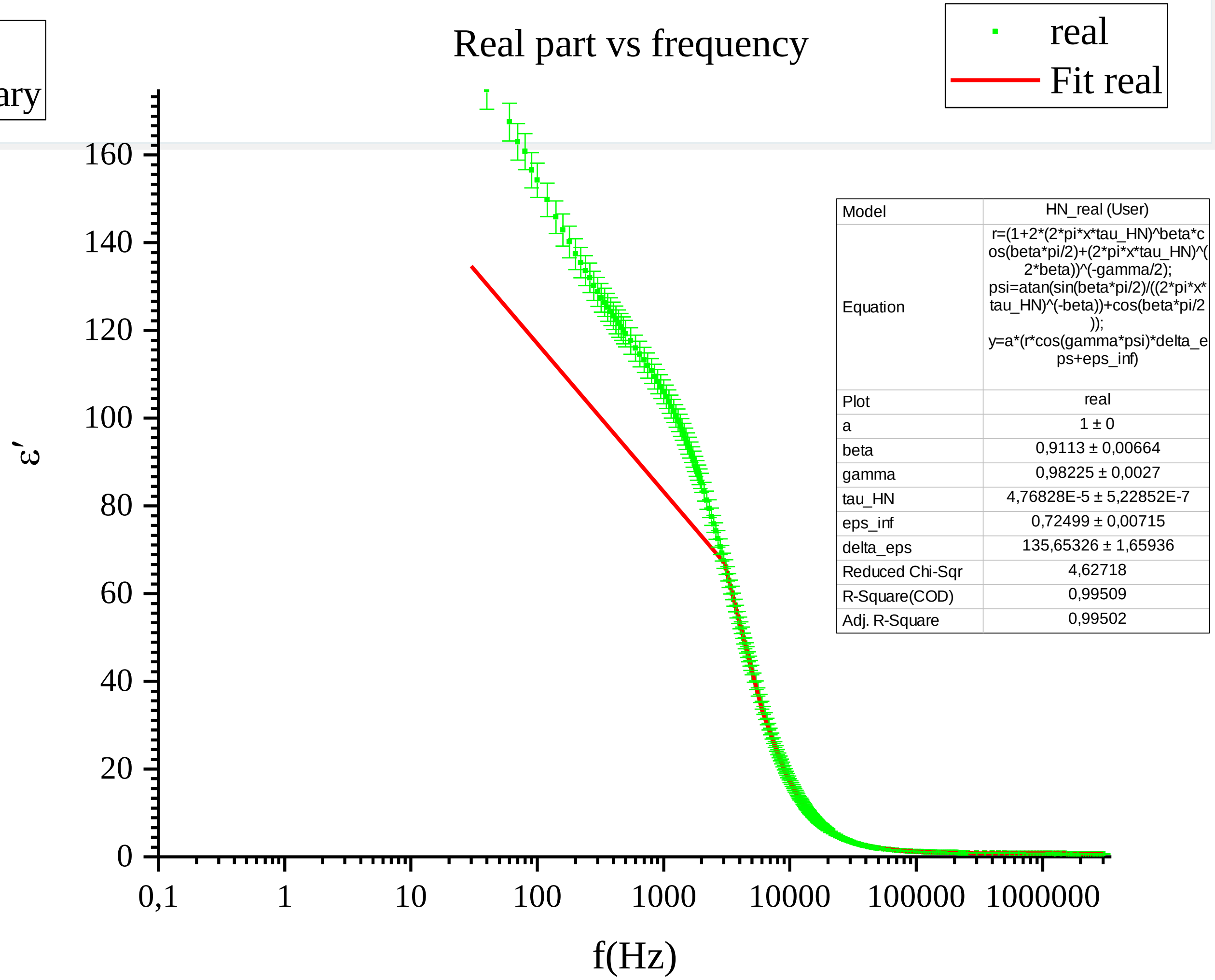

Global fit – No corrections

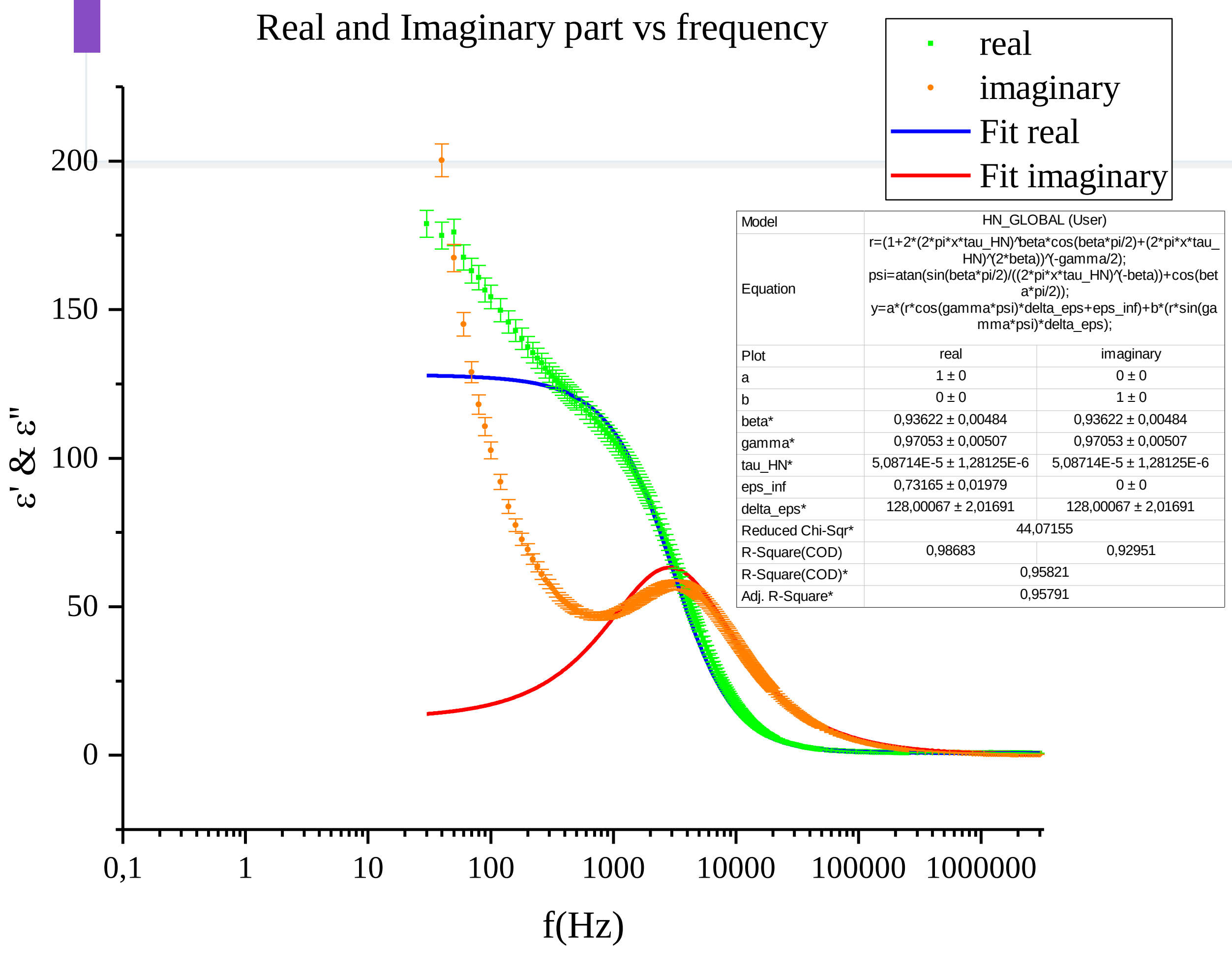

Model	HN_GLOBAL (User)	
Equation	r=(1+2*(2*pi*x*tau_HN)^beta*cos(beta*pi/2)+(2*pi*x*tau_HN)^(2*beta))^(-gamma/2); psi=atan(sin(beta*pi/2)/((2*pi*x*tau_HN)^(-beta))+cos(beta*pi/2)); y=a*(r*cos(gamma*psi)*delta_eps+eps_inf)+b*(r*sin(gamma*psi)*delta_eps);	
Plot	real	imaginary
a	1 ± 0	0 ± 0
b	0 ± 0	1 ± 0
beta*	0,93622 ± 0,00484	0,93622 ± 0,00484
gamma*	0,97053 ± 0,00507	0,97053 ± 0,00507
tau_HN*	5,08714E-5 ± 1,28125E-6	5,08714E-5 ± 1,28125E-6
eps_inf	0,73165 ± 0,01979	0 ± 0
delta_eps*	128,00067 ± 2,01691	128,00067 ± 2,01691
Reduced Chi-Sqr*	44,07155	
R-Square(COD)	0,98683	0,92951
R-Square(COD)*	0,95821	
Adj. R-Square*	0,95791	

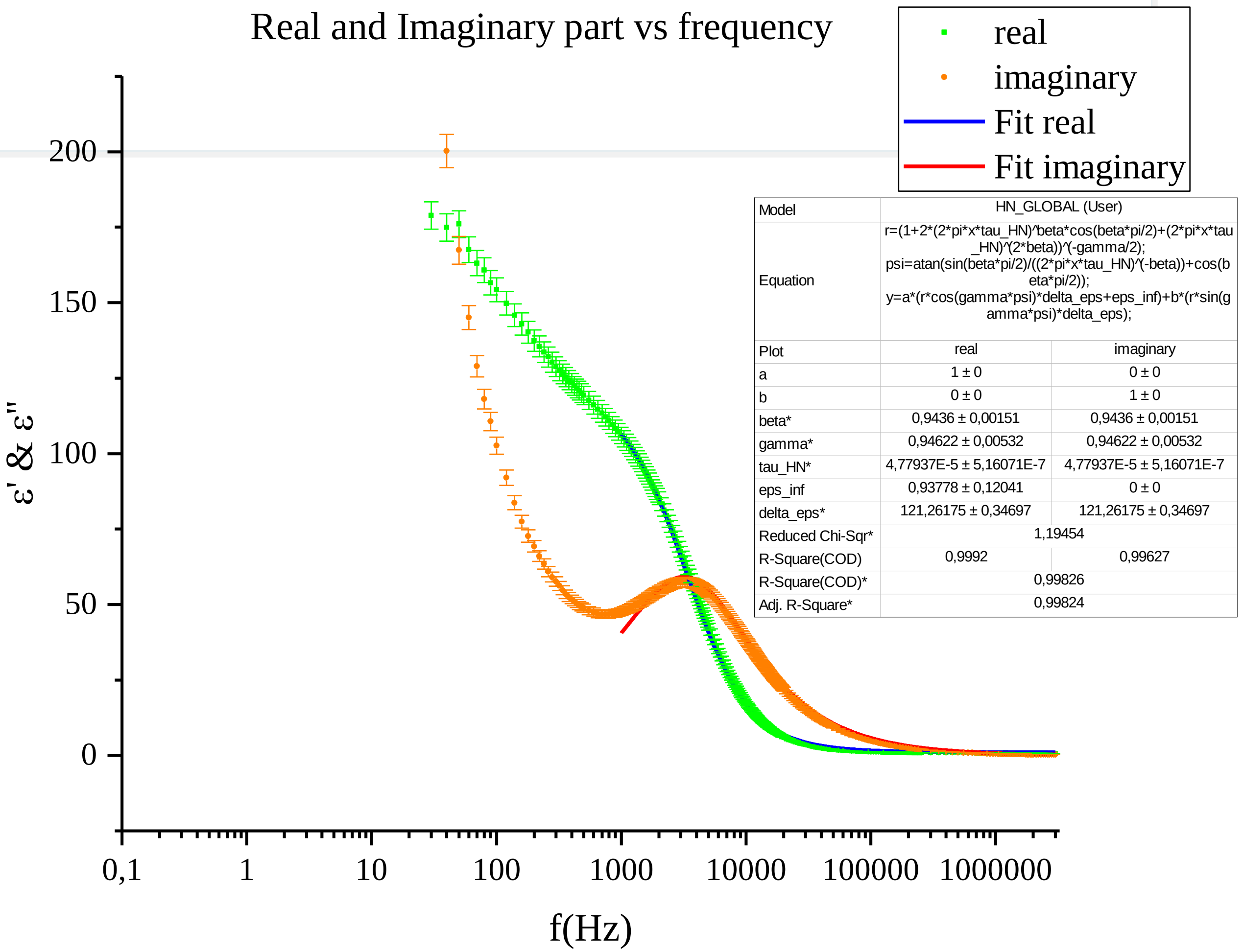

Model	HN_GLOBAL (User)	
Equation	r=(1+2*(2*pi*x*tau_HN)^beta*cos(beta*pi/2)+(2*pi*x*tau_HN)^(2*beta))^(-gamma/2); psi=atan(sin(beta*pi/2)/((2*pi*x*tau_HN)^(-beta))+cos(beta*pi/2)); y=a*(r*cos(gamma*psi)*delta_eps+eps_inf)+b*(r*sin(gamma*psi)*delta_eps);	
Plot	real	imaginary
a	1 ± 0	0 ± 0
b	0 ± 0	1 ± 0
beta*	0,9436 ± 0,00151	0,9436 ± 0,00151
gamma*	0,94622 ± 0,00532	0,94622 ± 0,00532
tau_HN*	4,77937E-5 ± 5,16071E-7	4,77937E-5 ± 5,16071E-7
eps_inf	0,93778 ± 0,12041	0 ± 0
delta_eps*	121,26175 ± 0,34697	121,26175 ± 0,34697
Reduced Chi-Sqr*	1,19454	
R-Square(COD)	0,9992	0,99627
R-Square(COD)*	0,99826	
Adj. R-Square*	0,99824	

Global fits with real and imaginary corrections

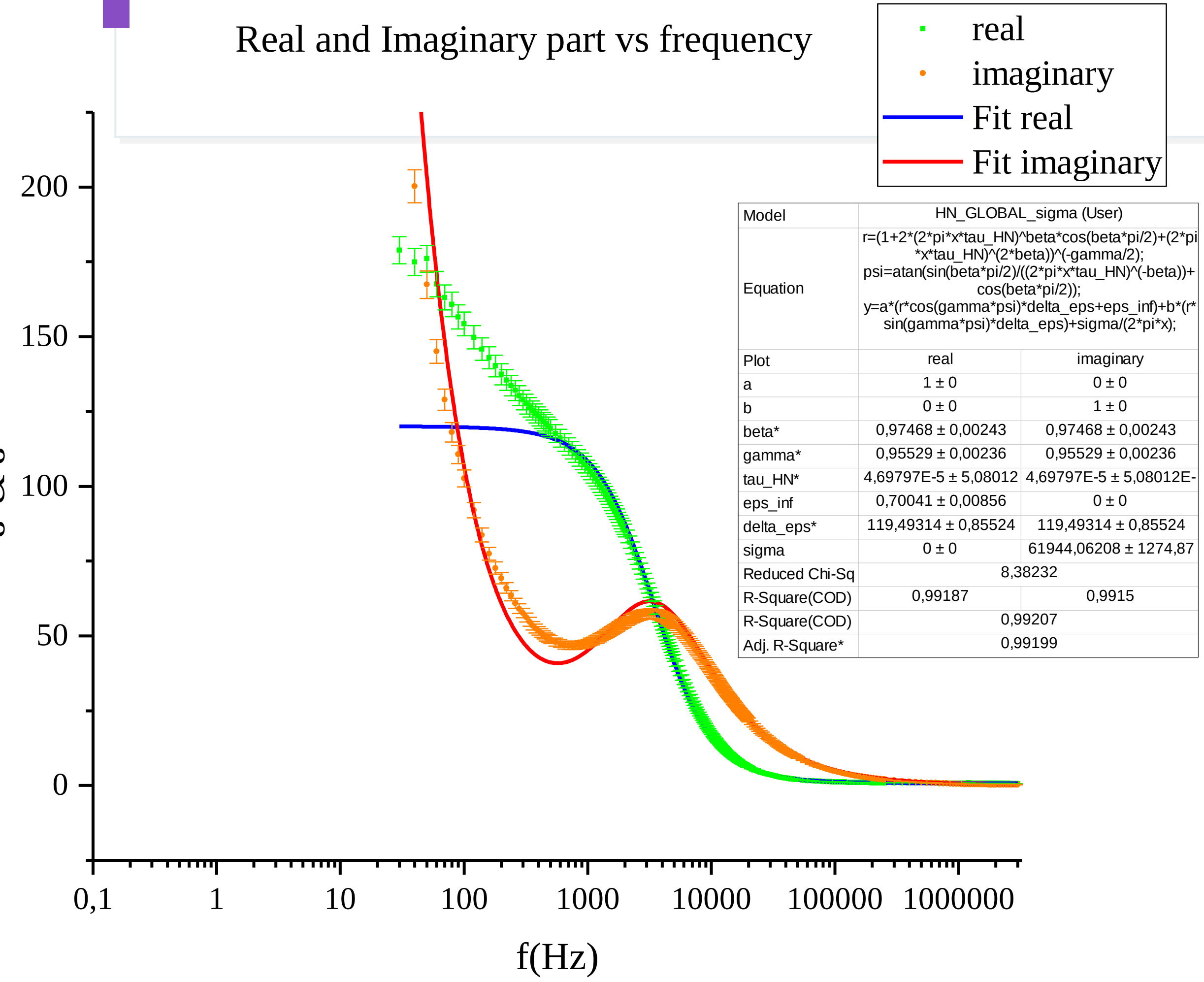

Model	HN_GLOBAL_sigma (User)	
Equation	r=(1+2*(2*pi*x*tau_HN)^beta*cos(beta*pi/2)+(2*pi*x*tau_HN)^(2*beta))^(-gamma/2); psi=atan(sin(beta*pi/2)/((2*pi*x*tau_HN)^(-beta))+cos(beta*pi/2)); y=a*(r*cos(gamma*psi)*delta_eps+eps_inf)+b*(r*sin(gamma*psi)*delta_eps)+sigma/(2*pi*x);	
Plot	real	imaginary
a	1 ± 0	0 ± 0
b	0 ± 0	1 ± 0
beta*	0,97468 ± 0,00243	0,97468 ± 0,00243
gamma*	0,95529 ± 0,00236	0,95529 ± 0,00236
tau_HN*	4,69797E-5 ± 5,08012	4,69797E-5 ± 5,08012E-
eps_inf	0,70041 ± 0,00856	0 ± 0
delta_eps*	119,49314 ± 0,85524	119,49314 ± 0,85524
sigma	0 ± 0	61944,06208 ± 1274,87
Reduced Chi-Sq	8,38232	
R-Square(COD)	0,99187	0,9915
R-Square(COD)	0,99207	
Adj. R-Square*	0,99199	

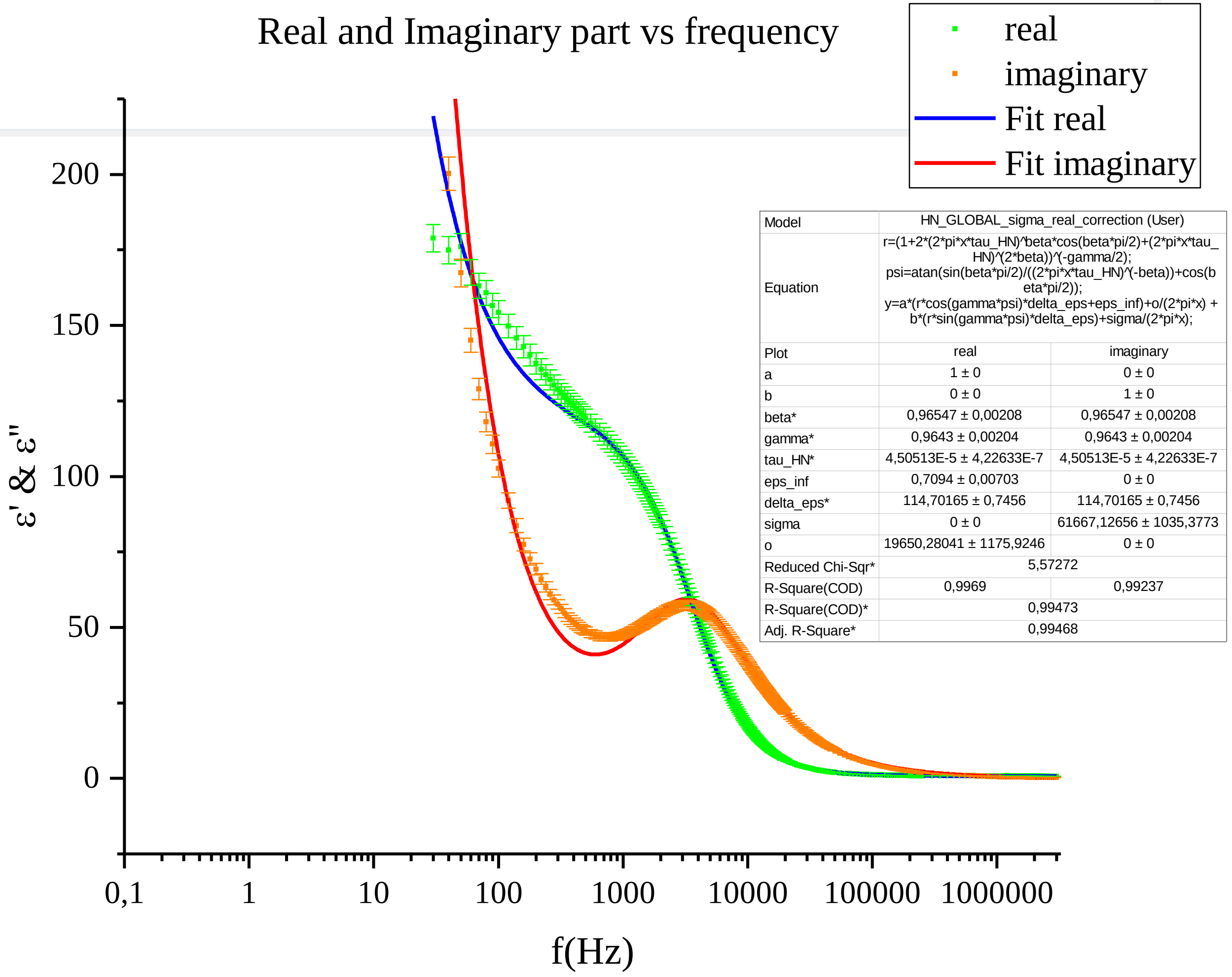

Model	HN_GLOBAL_sigma_real_correction (User)	
Equation	r=(1+2*(2*pi*x*tau_HN)^beta*cos(beta*pi/2)+(2*pi*x*tau_HN)^(2*beta))^(-gamma/2); psi=atan(sin(beta*pi/2)/((2*pi*x*tau_HN)^(-beta))+cos(beta*pi/2)); y=a*(r*cos(gamma*psi)*delta_eps+eps_inf)+o/(2*pi*x) + b*(r*sin(gamma*psi)*delta_eps)+sigma/(2*pi*x);	
Plot	real	imaginary
a	1 ± 0	0 ± 0
b	0 ± 0	1 ± 0
beta*	0,96547 ± 0,00208	0,96547 ± 0,00208
gamma*	0,9643 ± 0,00204	0,9643 ± 0,00204
tau_HN*	4,50513E-5 ± 4,22633E-7	4,50513E-5 ± 4,22633E-7
eps_inf	0,7094 ± 0,00703	0 ± 0
delta_eps*	114,70165 ± 0,7456	114,70165 ± 0,7456
sigma	0 ± 0	61667,12656 ± 1035,3773
o	19650,28041 ± 1175,9246	0 ± 0
Reduced Chi-Sqr*	5,57272	
R-Square(COD)	0,9969	0,99237
R-Square(COD)*	0,99473	
Adj. R-Square*	0,99468	

Global fit with corrections with exponents

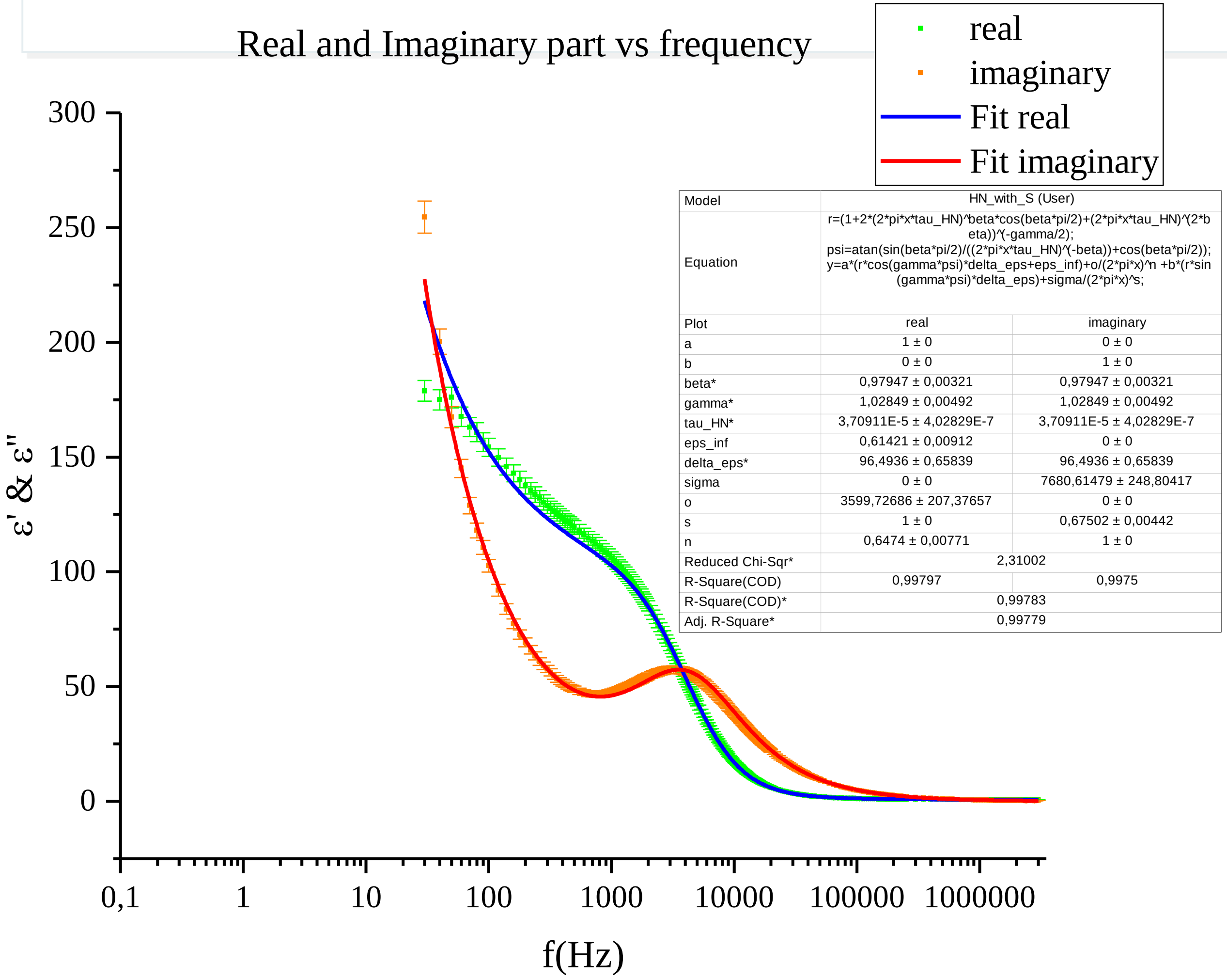

Model	HN_with_S (User)	
Equation	r=(1+2*(2*pi*x*tau_HN)^beta*cos(beta*pi/2)+(2*pi*x*tau_HN)^(2*beta))^(-gamma/2); psi=atan(sin(beta*pi/2)/((2*pi*x*tau_HN)^(-beta))+cos(beta*pi/2)); y=a*(r*cos(gamma*psi)*delta_eps+eps_inf)+o/(2*pi*x)^n +b*(r*sin(gamma*psi)*delta_eps)+sigma/(2*pi*x)^s;	
Plot	real	imaginary
a	1 ± 0	0 ± 0
b	0 ± 0	1 ± 0
beta*	0,97947 ± 0,00321	0,97947 ± 0,00321
gamma*	1,02849 ± 0,00492	1,02849 ± 0,00492
tau_HN*	3,70911E-5 ± 4,02829E-7	3,70911E-5 ± 4,02829E-7
eps_inf	0,61421 ± 0,00912	0 ± 0
delta_eps*	96,4936 ± 0,65839	96,4936 ± 0,65839
sigma	0 ± 0	7680,61479 ± 248,80417
o	3599,72686 ± 207,37657	0 ± 0
s	1 ± 0	0,67502 ± 0,00442
n	0,6474 ± 0,00771	1 ± 0
Reduced Chi-Sqr*	2,31002	
R-Square(COD)	0,99797	0,9975
R-Square(COD)*	0,99783	
Adj. R-Square*	0,99779	

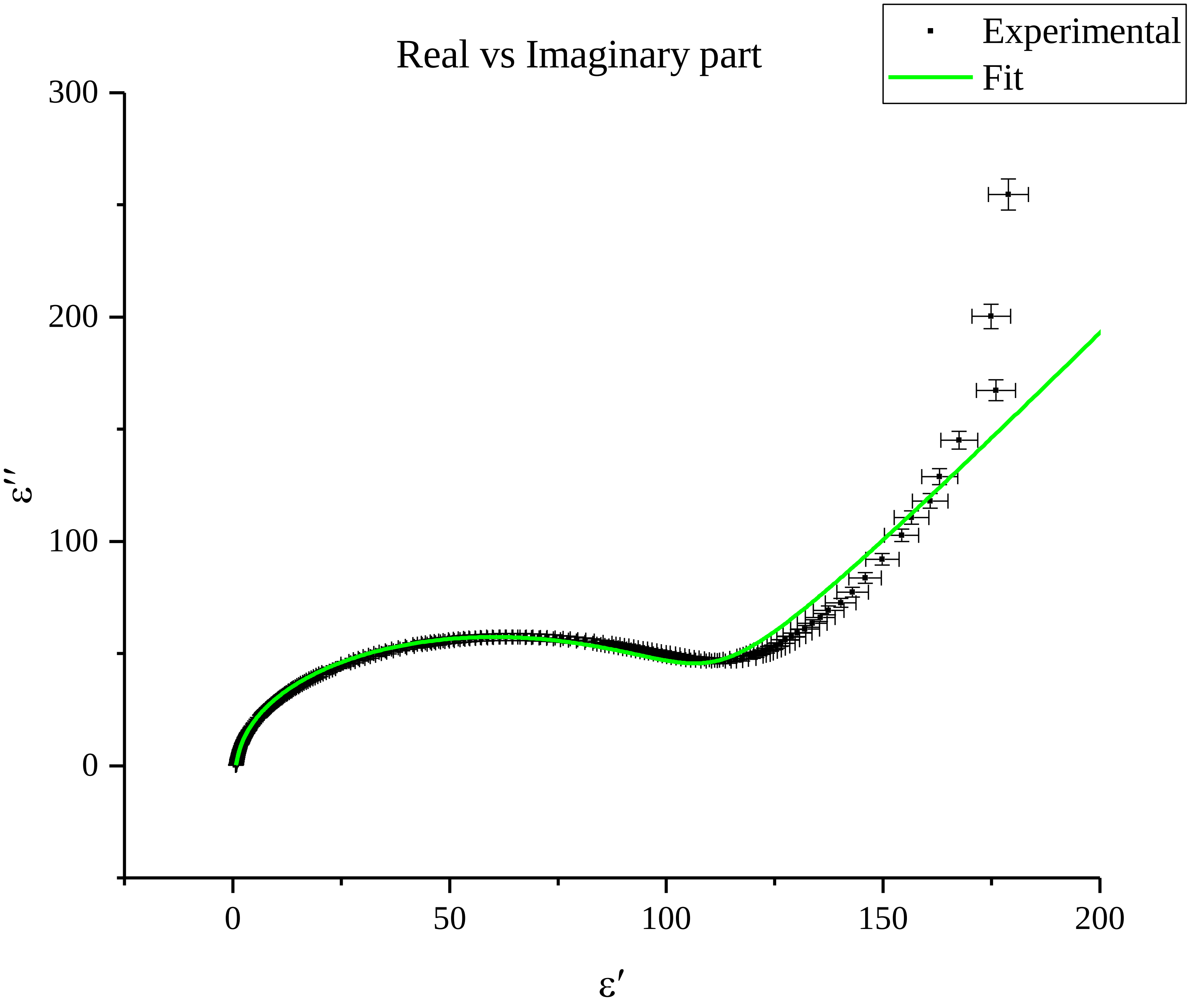
Real vs Imaginary part
Experimental
Fit
300
200
100
0
ε″
0
50
100
150
200
ε′

Parameter comparison

Fits / Parameters	without uncertainties and exponents	with uncertainties but without exponents	without uncertainties and with exponents	with uncertainties and exponents
$\sigma(\Omega\text{m})^{-1}$	$5{,}38 \times 10^{-8} \pm 8{,}31 \times 10^{-10}$	$5{,}48 \times 10^{-7} \pm 1{,}13 \times 10^{-8}$	$1{,}43 \times 10^{-7} \pm 3{,}97 \times 10^{-9}$	$6{,}80 \times 10^{-8} \pm 2{,}20 \times 10^{-9}$
ϵ_∞	$-0{,}39 \pm 0{,}49$	$0{,}70 \pm 0{,}01$	$-0{,}57 \pm 0{,}09$	$0{,}61 \pm 0{,}01$
β	$0{,}73 \pm 0{,}01$	$0{,}97 \pm 0{,}01$	$0{,}92 \pm 0{,}002$	$0{,}98 \pm 0{,}01$
τ_{HN}	$(9{,}22 + 1{,}45) \times 10^{-5}$	$4{,}70 \times 10^{-5} \pm 5{,}08 \times 10^{-7}$	$3{,}37 \times 10^{-5} \pm 4{,}51 \times 10^{-7}$	$3{,}71 \times 10^{-5} \pm 4{,}03 \times 10^{-7}$
$\Delta\epsilon$	$126{,}83 \pm 3{,}66$	$119{,}49 \pm 0{,}86$	$78{,}81 \pm 0{,}27$	$96{,}49 \pm 0{,}66$
$\mathcal{O}$	-------------------------	-------------------------	$673{,}41 \pm 19{,}68$	$3599{,}73 \pm 207{,}38$
s	-------------------------	-------------------------	$0{,}85 \pm 0{,}01$	$0{,}68 \pm 0{,}01$
n	-------------------------	-------------------------	$0{,}43 \pm 0{,}01$	$0{,}65 \pm 0{,}01$

Conclusions

Comparison of the fits

- Adding the Maxwell-Wagner and conductivity terms improved the fit to the data in the lower frequencies range.
- Comparing with the independent fit, the global fit has a better fit as indicated by the chi-squared.
- The global fit real part vs. frequency approaches the experimental data without uncertainties better than the data with uncertainty.

Comparison of the fits

- The global fit without uncertainties has a smaller chi-squared than with uncertainties, because in the latter the real part fit begins to diverge at lower frequencies.
- It’s might be due to the different weights of the different points that make the fit converge to another solution.

Possible Improvements

- Improvements in area measurements (higher resolution pictures for example)
- C and tan δ error only estimated

→Check manufacturer information of measuring devices

- Deviation of fit and data in the real part (low frequency range)

→ Add different terms to the equation? Would another model be more accurate for our sample?